Basic models, animations and unsolved problems in welding

T. DebRoy

- A basic heat conduction model – benefits and limitations
- Applications of heat transfer and fluid flow models
    - Unusual weld pool shapes
    - Weld surface profiles
    - Effect of surface active elements
    - Welding two plates with different sulfur contents
    - Uphill, downhill, tilted, L and V configurations
    - Weld metal composition change
    - Why Sievert's Law cannot be directly applied in welding
- Tailoring weld geometry

Thanks to: A. Kumar, W. Zhang, B. Ribic, C.H. Kim, W. Pitscheneder, G. G. Roy, A. Arora, S. Mishra, T. J. Lienert, P. A. A. Khan, X. He, T. A. Palmer, A. De

Basic models in welding

Models the essential physical processes

"Essential" => of interest to many for meaningful understanding of the process and the weld metal

- Heat transfer and melting
- Evaporation of elements & dissolution of gases
- Flow of liquid metal
- Solidification & structural changes
- Properties

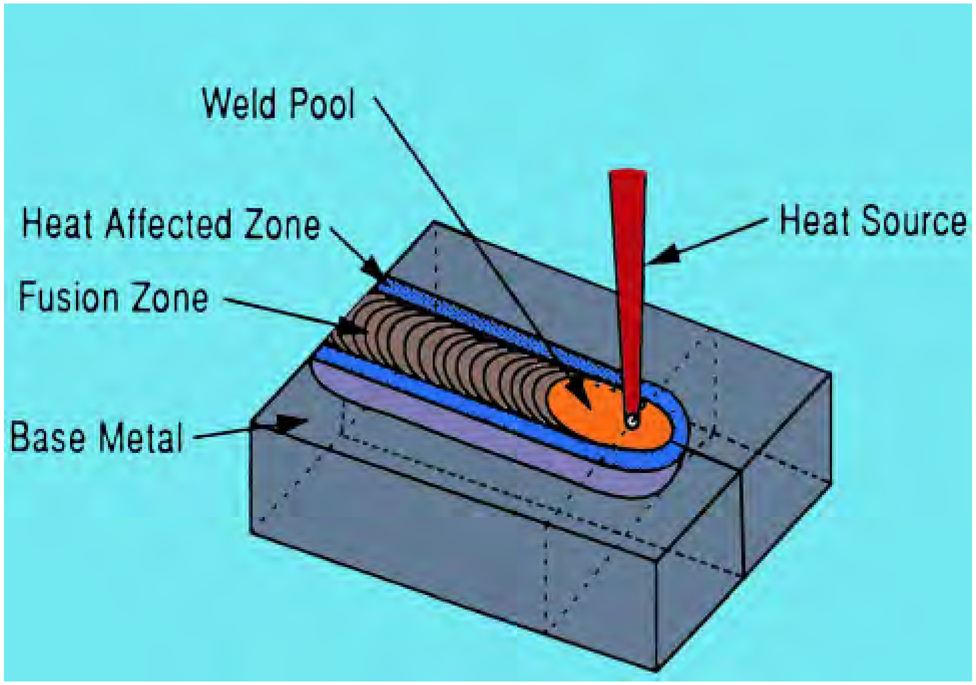

Rosenthal model for heat conduction in welding - a most widely used basic model

"For an engineer in search of a theory, the simpler the better"
(paraphrased)

Professor D. Brian Spalding

picture from http://www.cham.co.uk/about.php

Rosenthal model for heat conduction in welding

Analytical solution to calculate temperature fields, cooling rates and weld geometry

Widely used - simple, phenomenological and insightful

But ignores convection which is the main mechanism of heat transfer in many cases

Four main difficulties of heat conduction models

"Everything should be made as simple as possible,
but not simpler."

— Albert Einstein

From: http://rescomp.stanford.edu/~cheshire/EinsteinQuotes.html

Problem 1: diversity of weld shapes cannot be predicted from heat conduction equation

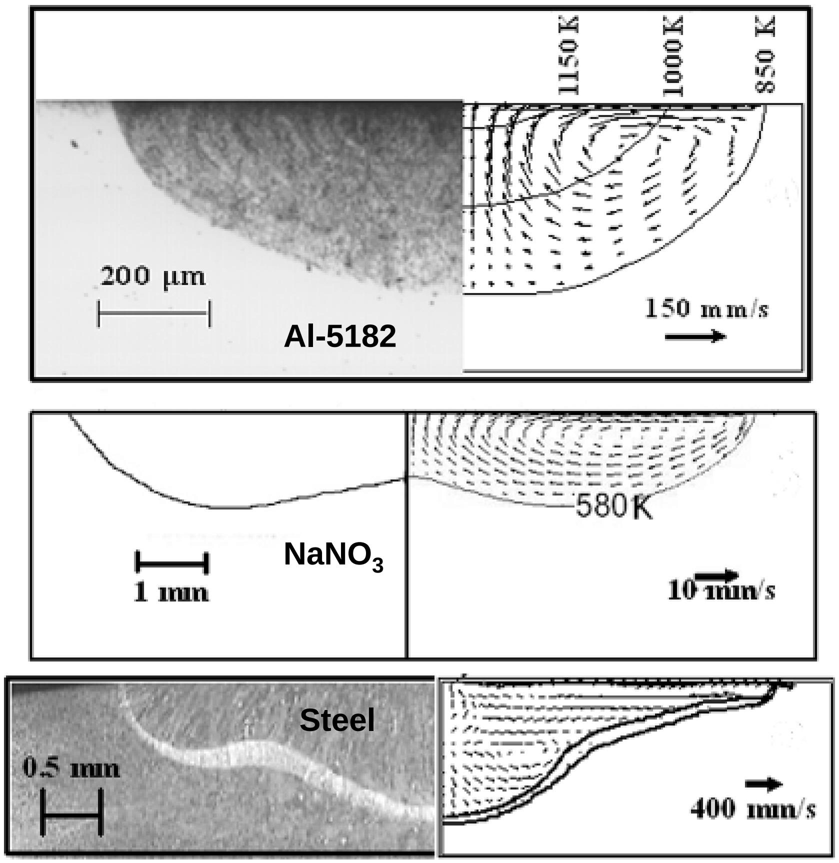

Laser beam welding

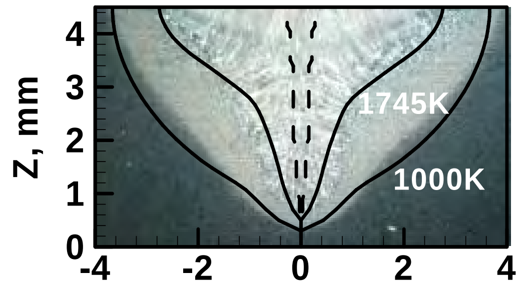

304 stainless
Laser-arc hybrid

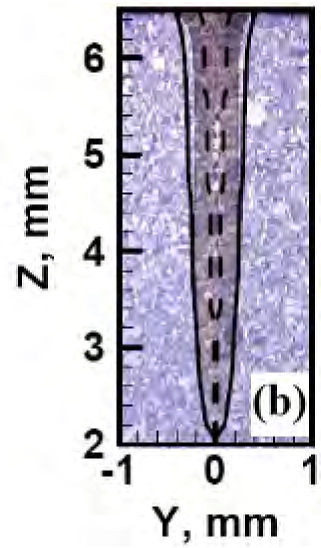

21Cr-6Ni-9Mn steel
Electron beam

Friction stir welding
Aluminum alloy AA2524

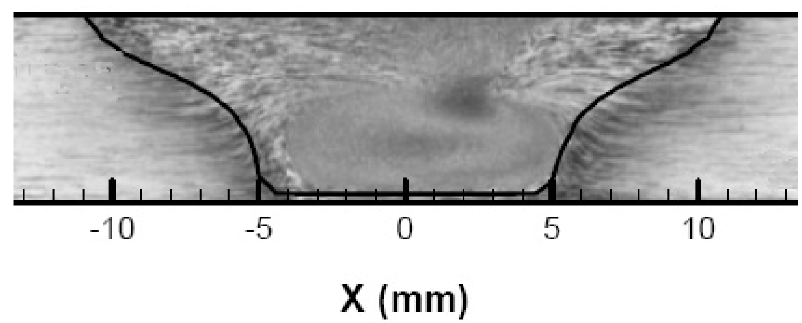

All these shapes have been explained considering convective heat transfer

Problem 2: weld orientation effect cannot be explained

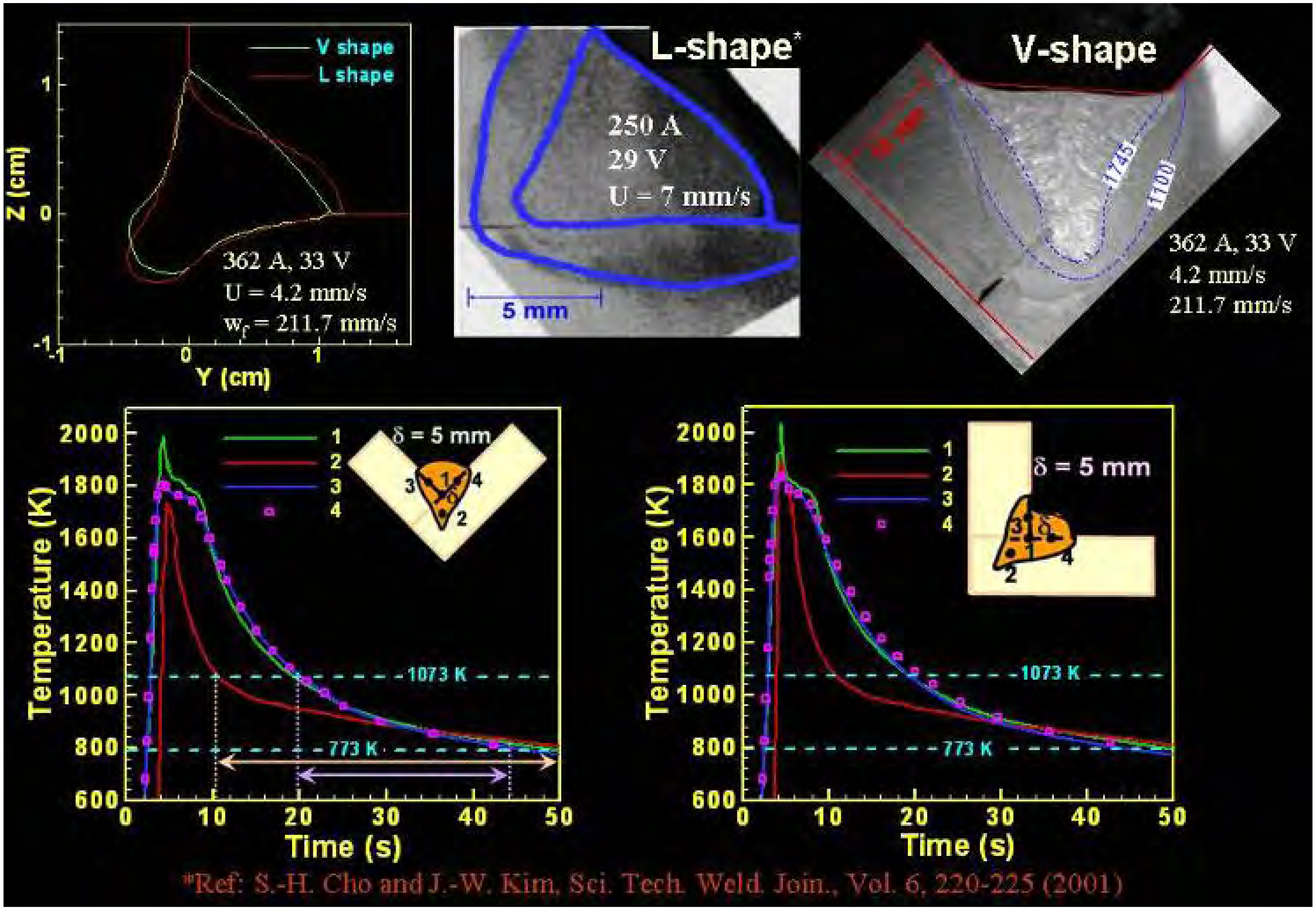

This effect has been explained considering convective heat transfer

Problem 3: The effects of minor alloying elements cannot be explained ignoring convection

20 ppm sulfur **150 ppm sulfur**

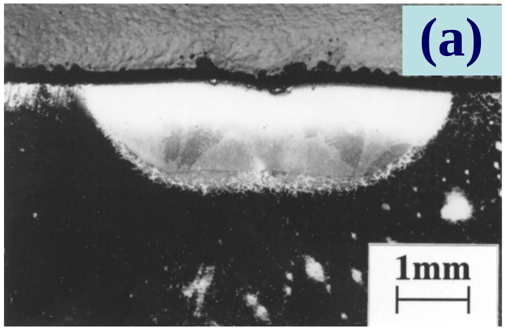

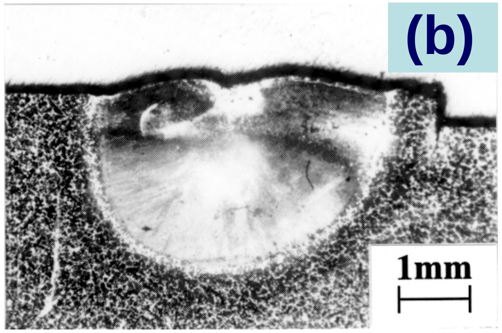

5200 W

*** Minor changes in composition => major changes in geometry**
*** Does not always happen!**

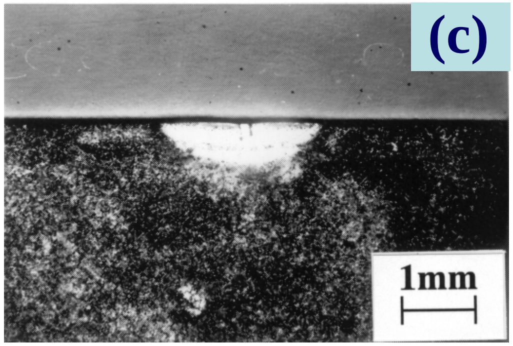

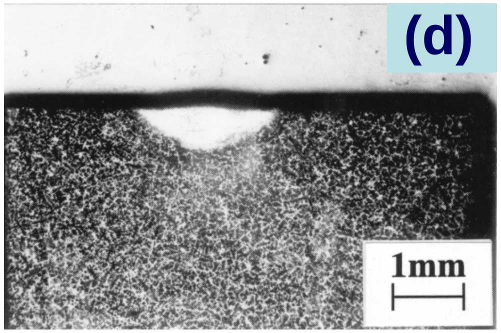

1900 W

The effects of oxygen and sulfur has been explained considering convective heat transfer

Problem 4: Heat conduction equations overpredict cooling rates

"…the heat conduction equation has been found to be inadequate in representing experimental cooling curves" SVENSSON, GRETOFT and BHADESHIA, An analysis of cooling curves from the fusion zone of steel weld deposits, *Scand. J. Metallurgy*, vol. 15, pp. 97-103, 1986.

They recommended use of empirical correlations

The heat conduction equations predict high temperature gradients and cooling rates because mixing of hot and cold liquids is ignored.

Convective heat transfer calculations do not have any such problems.

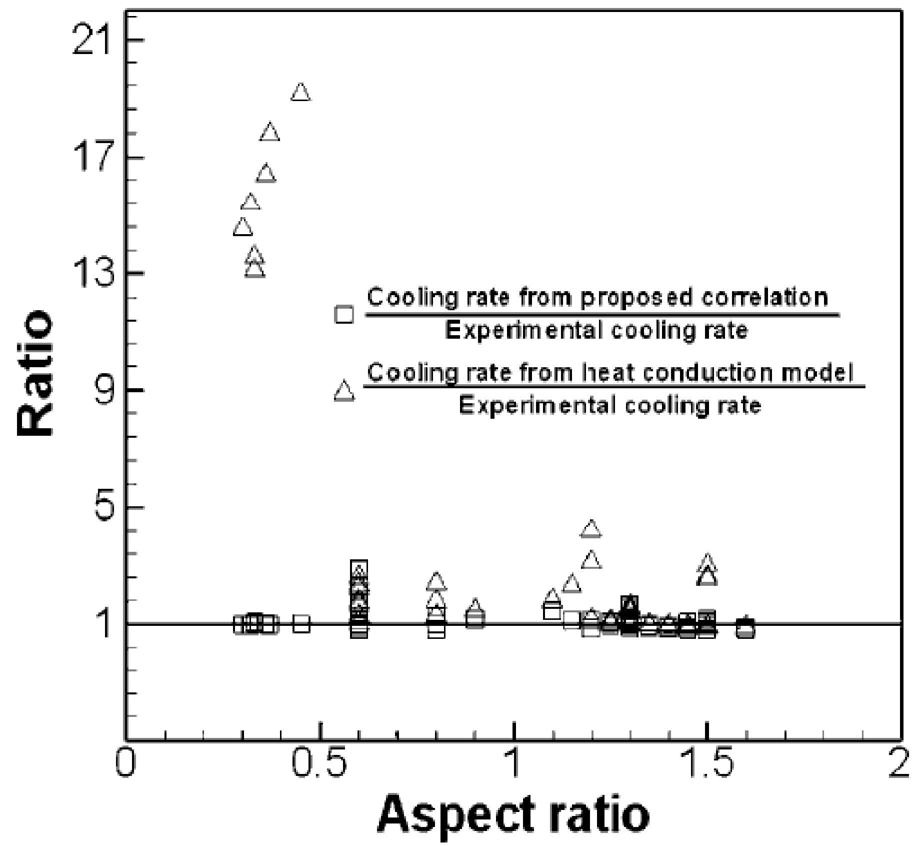

Heat and fluid flow models and their diverse applications

GTA weld pool with deformed free surface

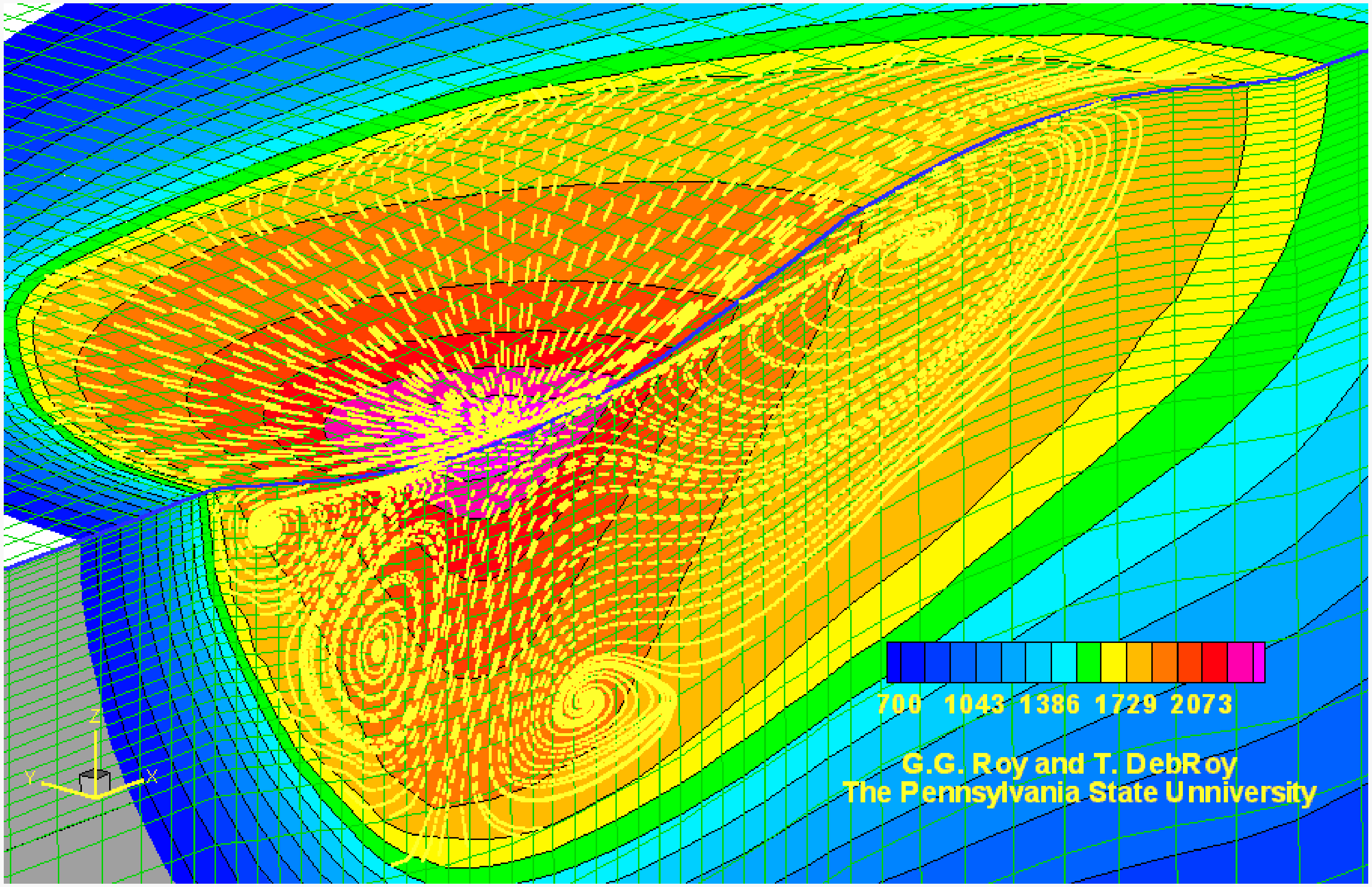

Heat and fluid flow models - diverse applications

Welding Processes

Gas tungsten arc (GTA), Gas metal arc (GMA), Laser (conduction & keyhole), Electron beam, GTA-Laser hybrid, Friction stir welding

The Main Engine

Transient, three dimensional, heat, mass and momentum transfer numerical model

Output

- Solidification parameters, solidification growth rates, temperature gradients etc.
- Transient temperature and velocity fields, mixing of consumables, heating and cooling rates, weld geometry
- Deformed free surface, loss of alloying elements, composition change etc.

Applications

Phase transformation in the fusion and heat affected zone
Grain growth in the heat affected zone
Inclusion type, size and distribution
Pore structure, gas dissolution etc

Many more applications

1. Fusion zone (FZ) and heat affect zone (HAZ) geometries
2. Grain size and topological features in the HAZ
3. Evolution of inclusion composition and size distribution
4. Evolution of microstructure in both FZ and HAZ
5. Control of cooling rates
6. Composition change owing to selective vaporization of alloying elements
7. Control of hydrogen and nitrogen in steel weldments
8. Joining of dissimilar materials including steels of different surface active elements such as sulfur and oxygen
9. Prevention of macro-porosity in laser welding
10. Enhancing fatigue property through improved surface finishing

1. Understanding unusual weld pool shapes

Wavy weld pool boundary

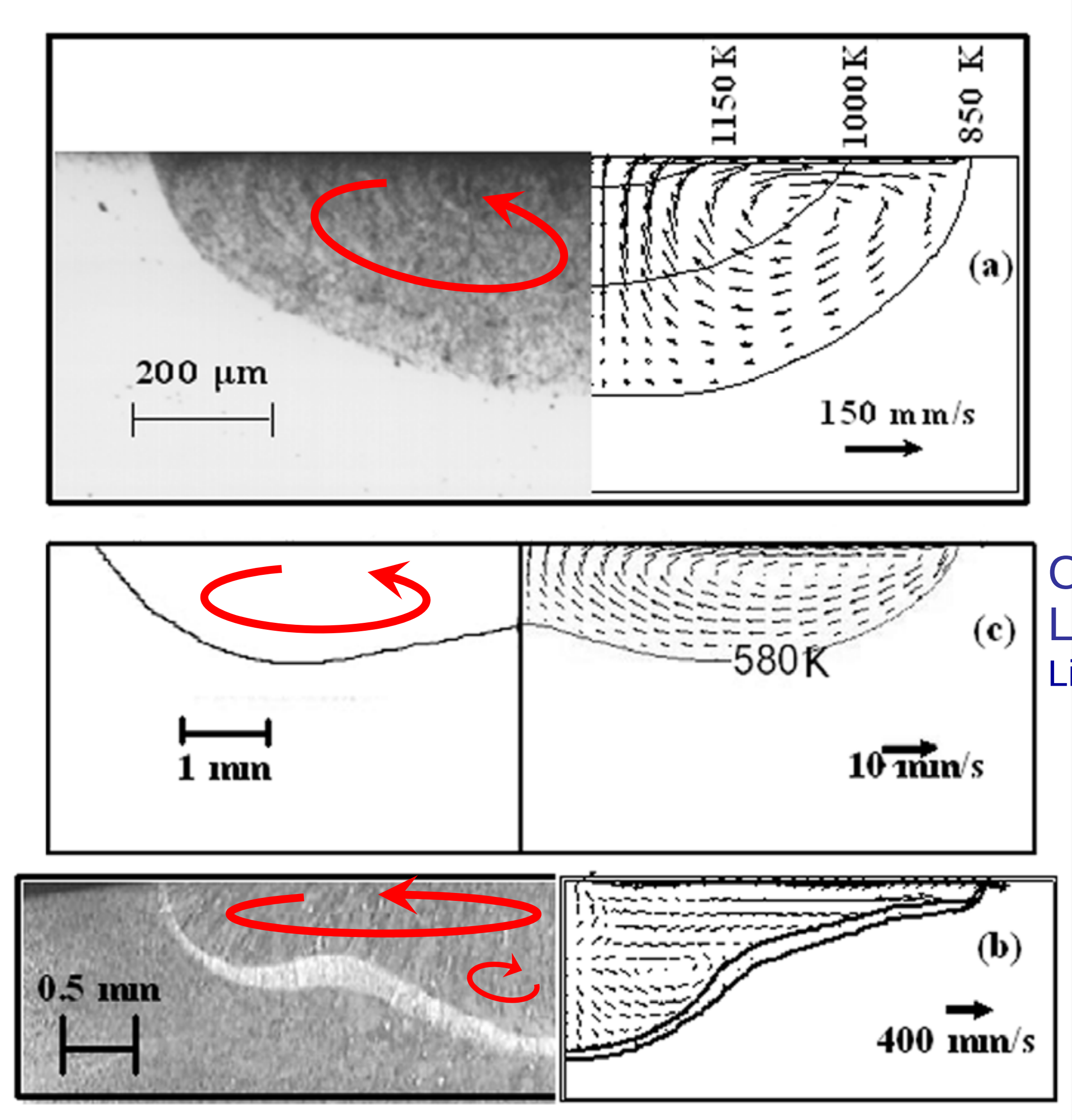

Hemispherical boundary
Arc welding of Al 5182
Zhao, DebRoy, Met. Trans B, 2001

Concave at the center
Laser melting of NaNO3
Limmaneevichitr, Kou, Welding Journal, 2000

Convex at the center
Arc welding of steel
Elmer, Palmer, Zhang, DebRoy, STWJ, 2008

Arora, Roy, and DebRoy, Scripta Materialia, 2009

Wavy weld pool boundary

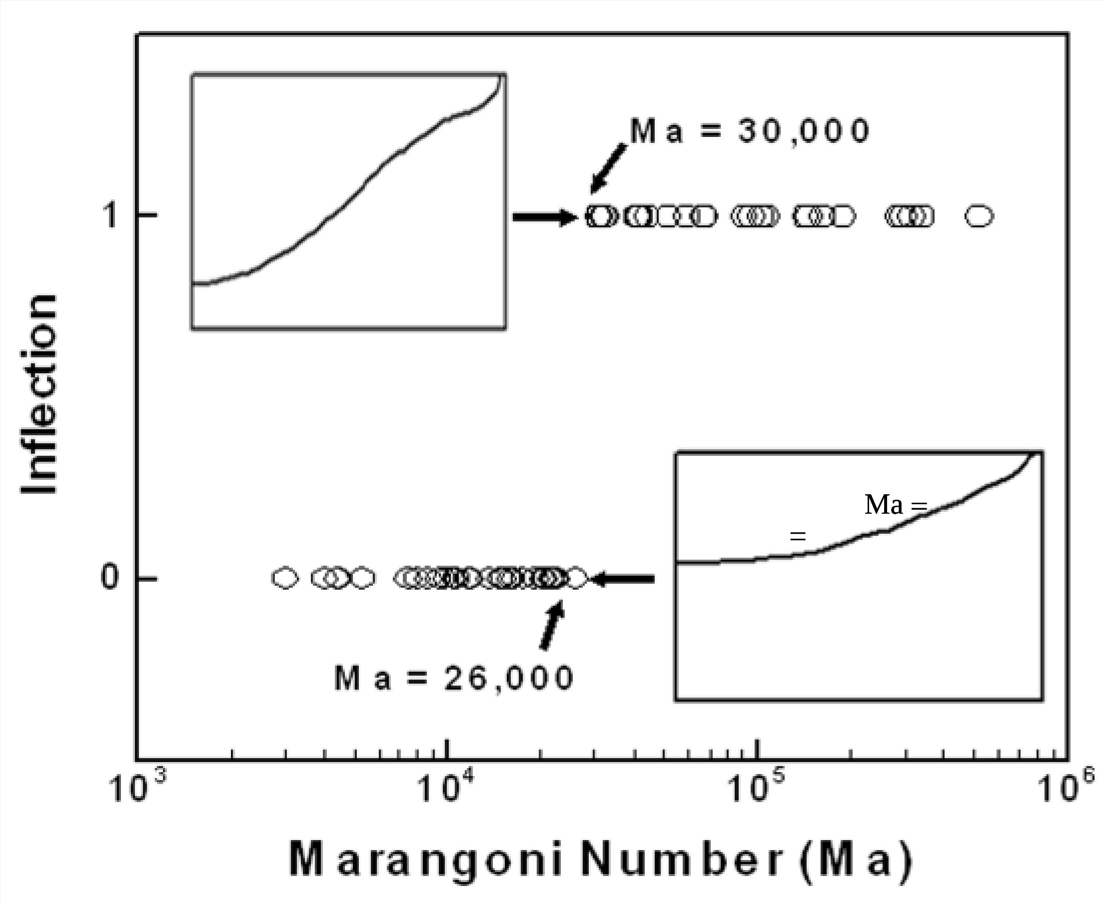

$$Ma = \frac{\text{Surface tension force}}{\text{Viscous force}}$$

$$= \frac{L\Delta T\,(d\gamma / dT)}{\alpha\mu}$$

L	Characteristic length
ΔT	Temperature difference
$d\gamma/dT$	First derivative of surface tension wrt temperature
α	Thermal diffusivity
μ	Viscosity

High Marangoni number, Ma, leads to formation of wavy weld pool boundary

Arora, Roy, and DebRoy, Scripta Materialia, 2009

Origin of wavy weld pool boundary

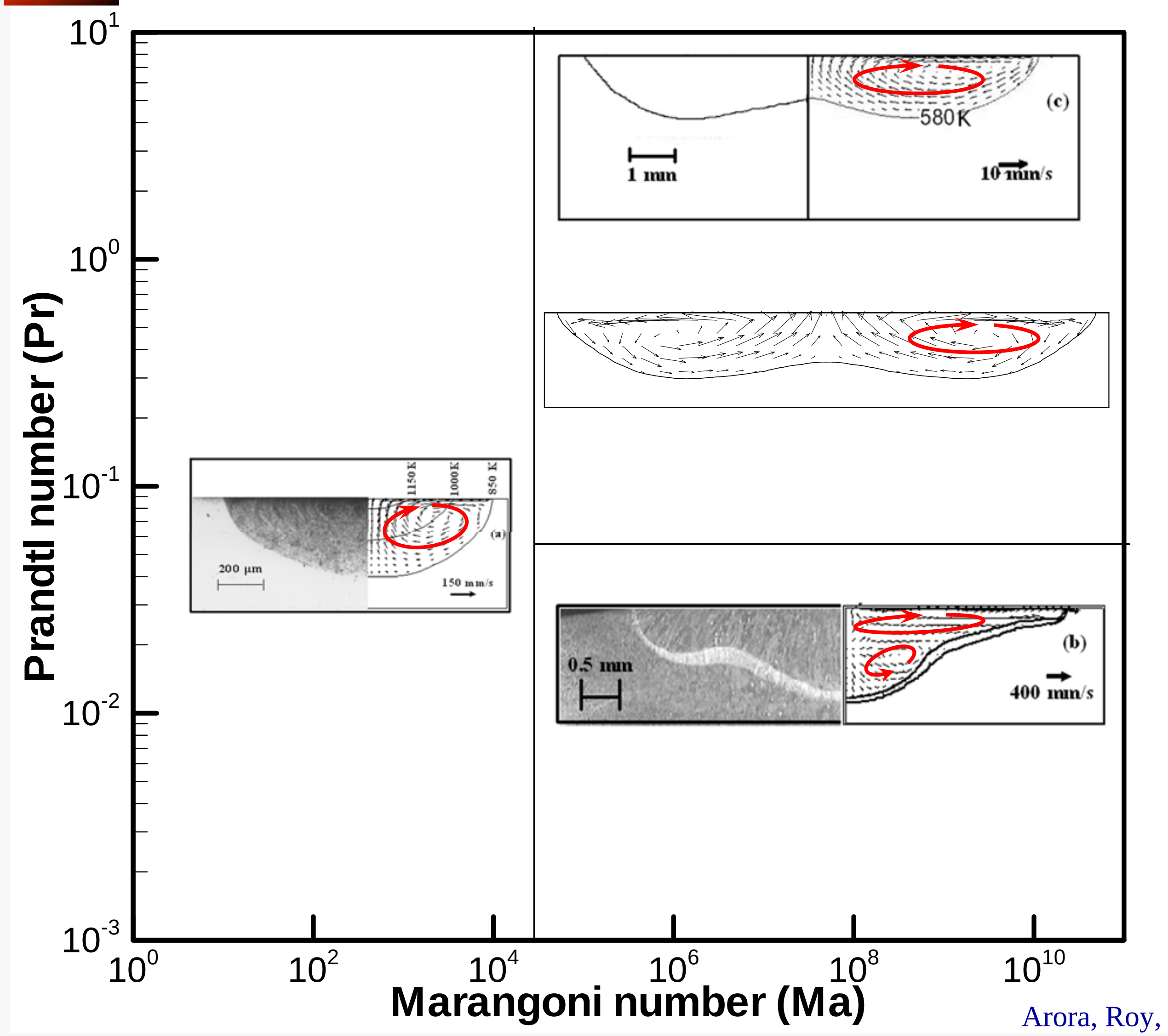

Marangoni (Ma) and Prandtl (Pr) numbers can be used to predict the shape of the wavy weld pool boundary

$$Ma = \frac{\text{Surface tension force}}{\text{Viscous force}}$$

$$Pr = \frac{\text{Viscous diffusion rate}}{\text{Thermal diffusion rate}}$$

Arora, Roy, and DebRoy, Scripta Materialia, 2009

2. Surface profiles

Why study surface profile?

Improper parameters $\Rightarrow$ poor mechanical properties $\Rightarrow$ defects $\Rightarrow$ failure

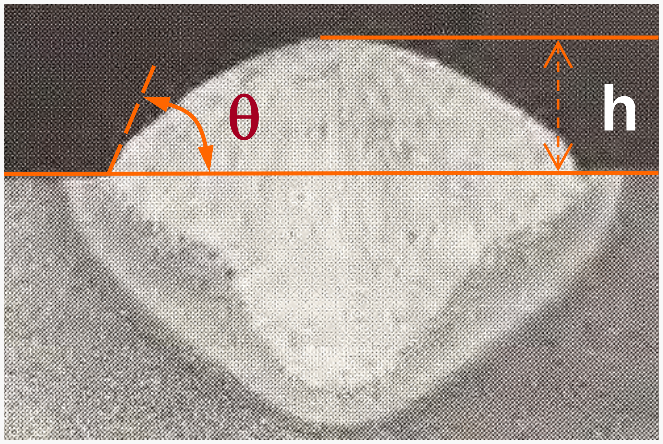

θ - weld toe angle
h - weld reinforcement height

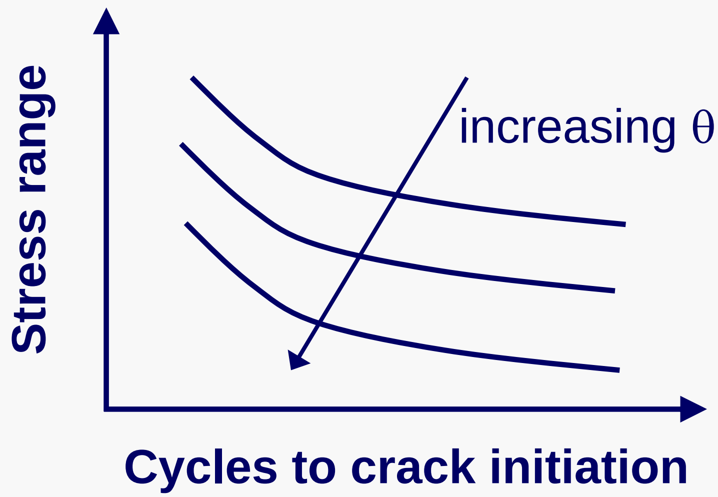

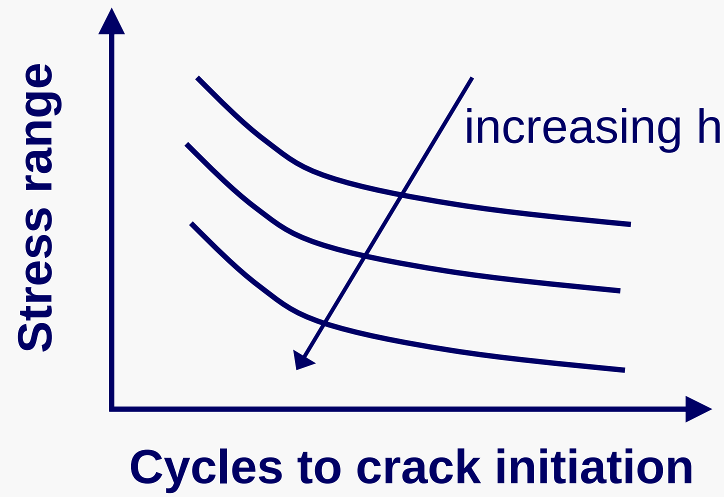

Development of bead profile in GMA welds

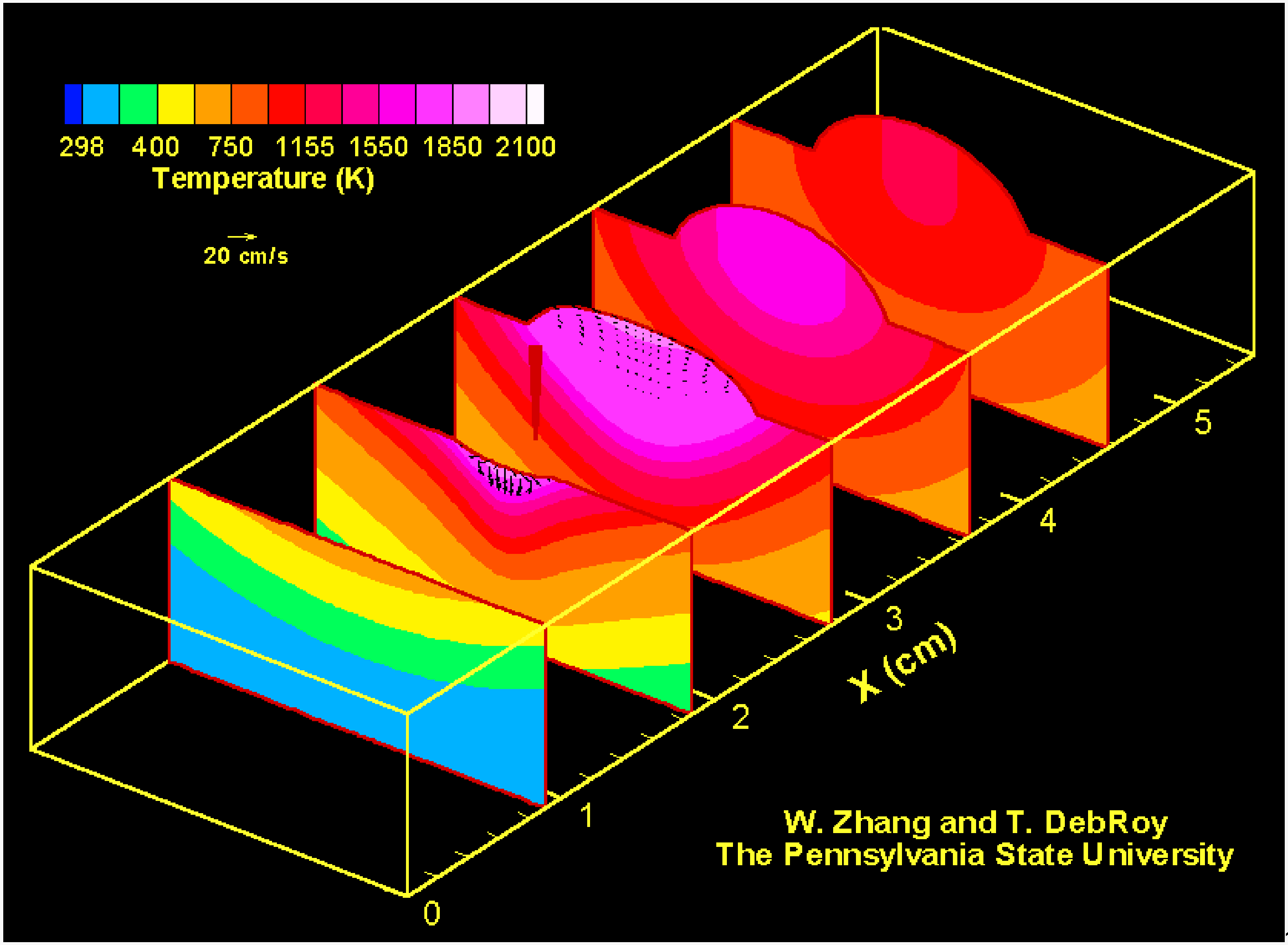

Calculated and experimental GMA bead shape

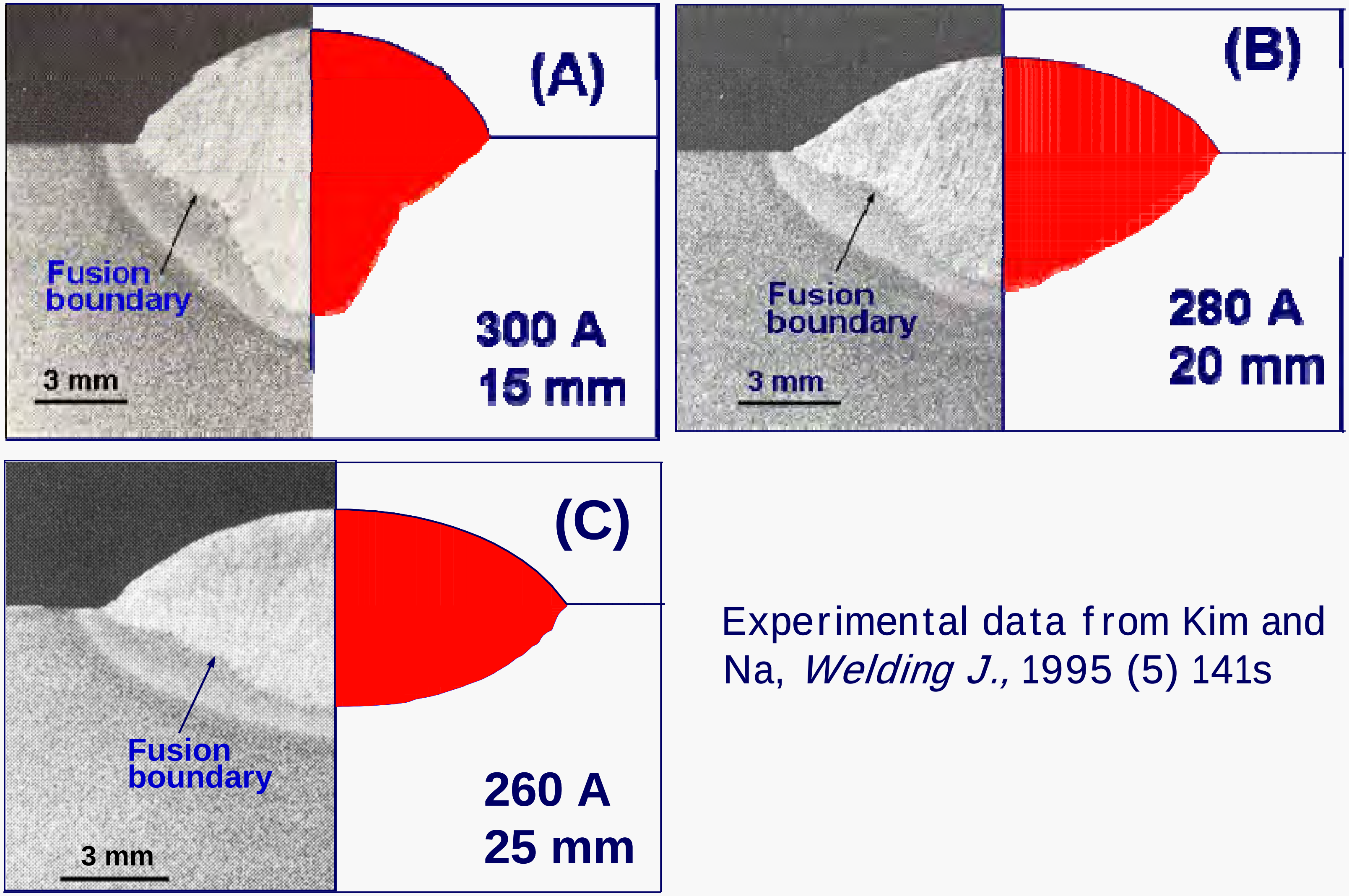

Experimental data from Kim and Na, *Welding J.,* 1995 (5) 141s

Effect of welding parameters on the solidified surface profile

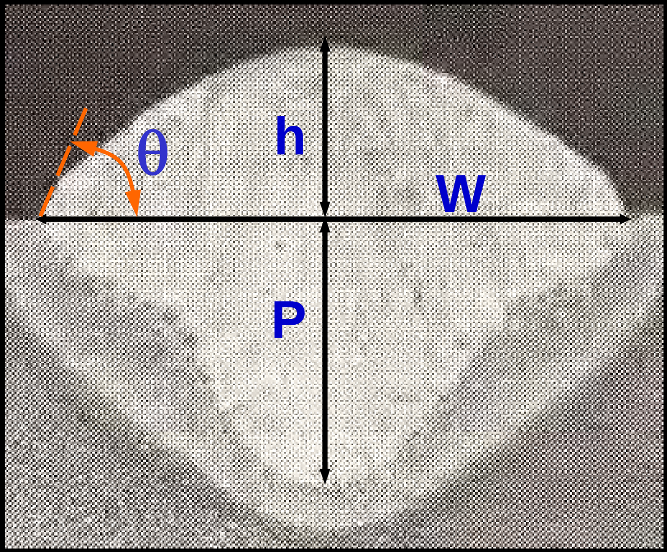

	Test case A (300 A, 15 mm)		Test case B (280 A, 20 mm)		Test case C (260 A, 25 mm)	
	Calc.	*Exp.*	Calc.	*Exp.*	Calc.	*Exp.*
Bead width (mm) - W	11.20	*11.32*	12.82	*12.60*	13.24	*13.20*
Bead Height (mm) – h	3.02	*3.12*	2.80	*2.82*	2.80	*2.79*
Penetration (mm) – P	5.00	*5.05*	4.00	*3.95*	2.90	*2.84*
Toe angle - θ	59^o	*53^o*	50^o	*47^o*	49^o	*49^o*

3. Effect of surface active elements

Convection in Fe and Fe-S Melts

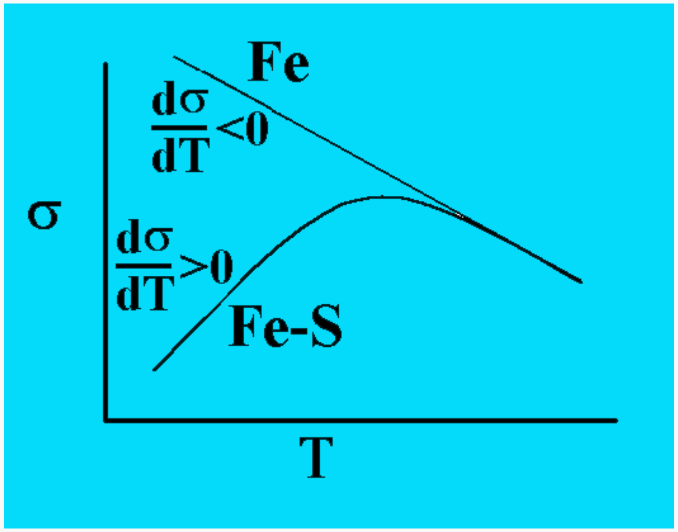

$$\tau = \frac{d\sigma}{dx} = \frac{d\sigma}{dT} \cdot \frac{dT}{dx}$$

Negative or positive

Negative

$$\mu \frac{\partial u}{\partial z} = f_L \left(\frac{\partial \gamma}{\partial T} \frac{\partial T}{\partial x} + \frac{\partial \gamma}{\partial C} \frac{\partial C}{\partial x} \right)$$

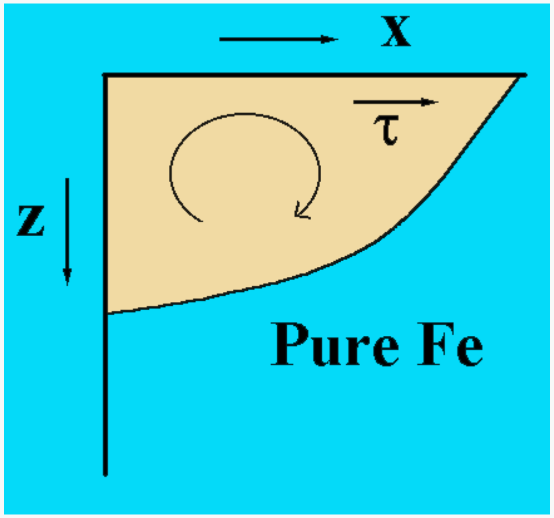

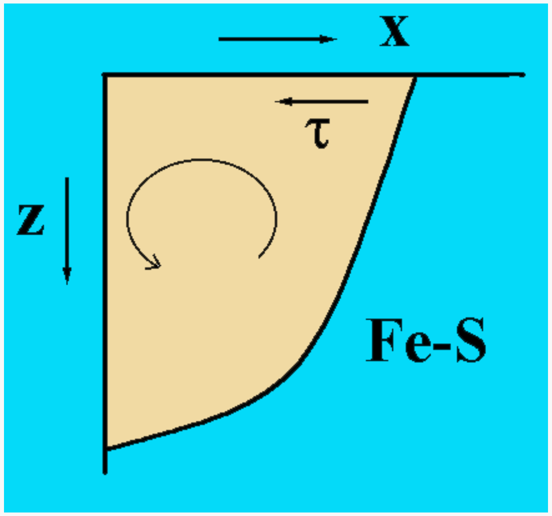

High power welding - sulfur affects penetration

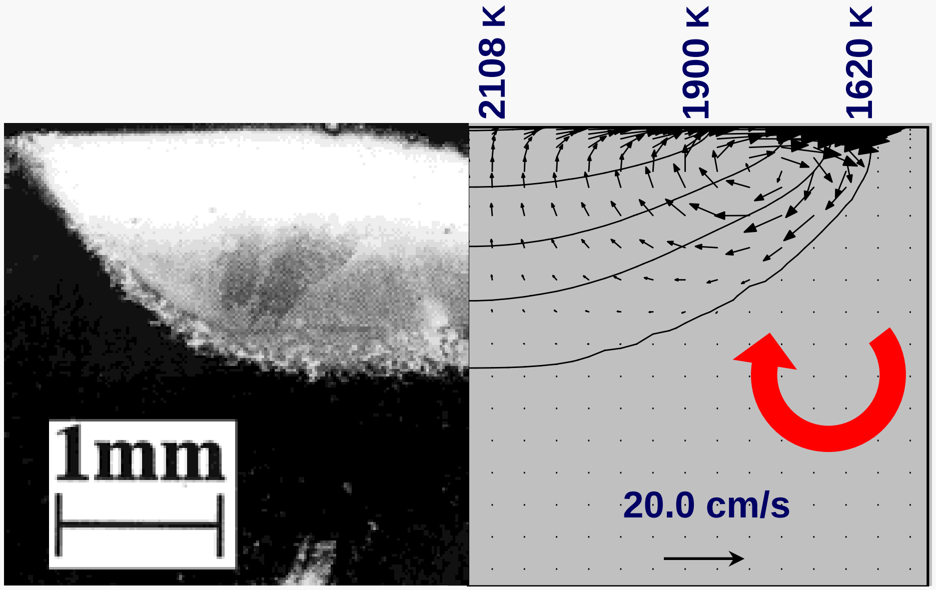

20 ppm sulfur

5200 W
Pe >> 80

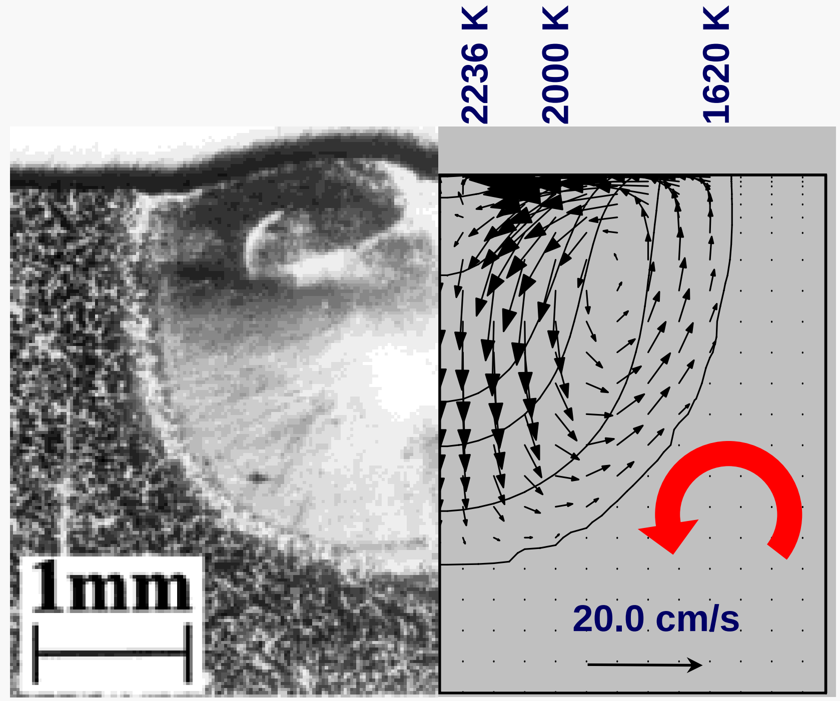

150 ppm sulfur

Minor changes in composition →
major changes in geometry

Low power welding - sulfur does not influence penetration

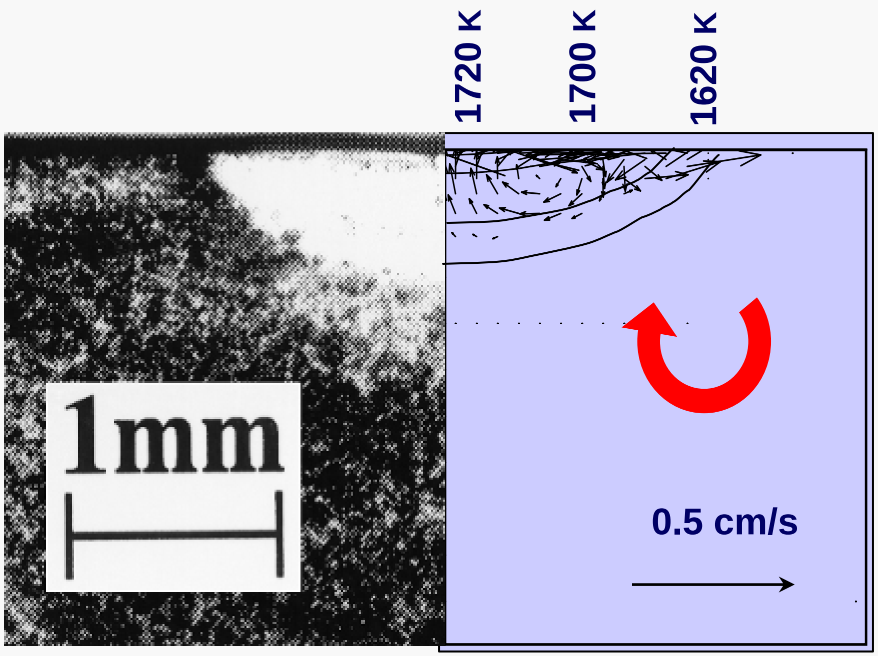

20 ppm sulfur

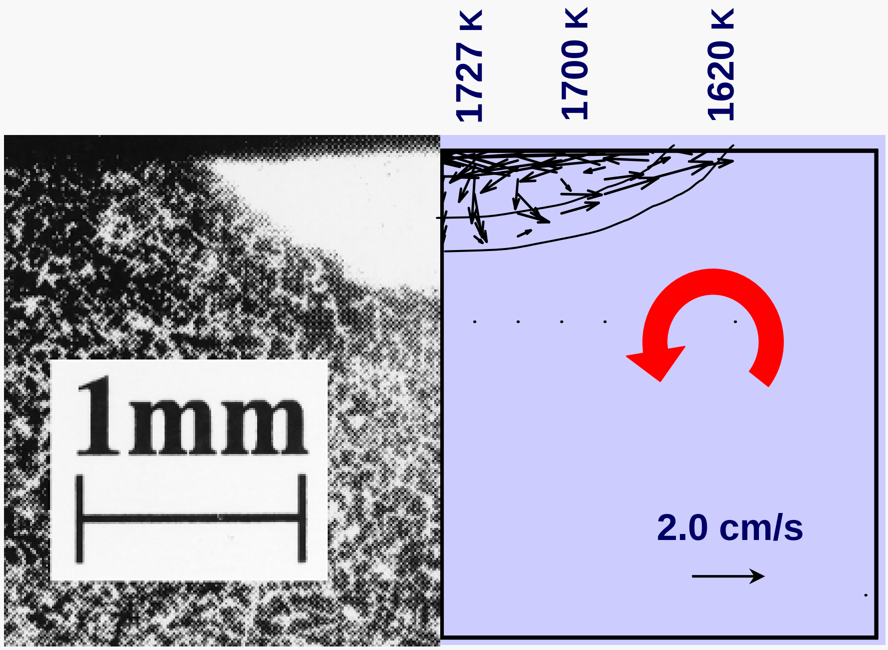

150 ppm sulfur

1900 W

Pe << 1

Minor change in composition →
Insignificant change in geometry

Variable penetration - summary

Experiments

- *reveal* what happens: *sometimes* the depth changes with % S
- but do not reveal why

Modeling

- surface active elements improve penetration *only when* convection is important (high Pe)

Modeling is a path to understand the science of welding

4. Welding two plates with different sulfur contents

Identifying factors affecting weld pool geometry

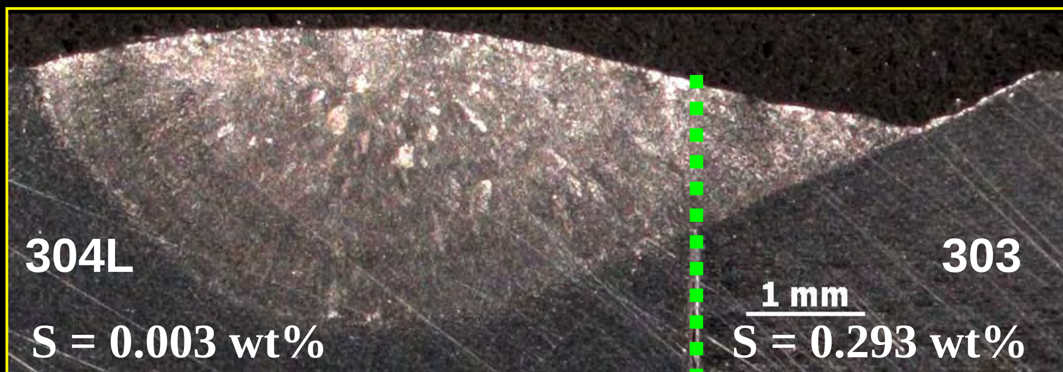

I = 150 A, V = 10.5 V, Welding speed = 1.7 mm/s

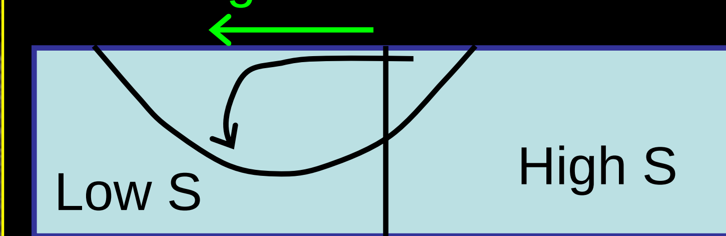

Distribution of sulfur on the top surface

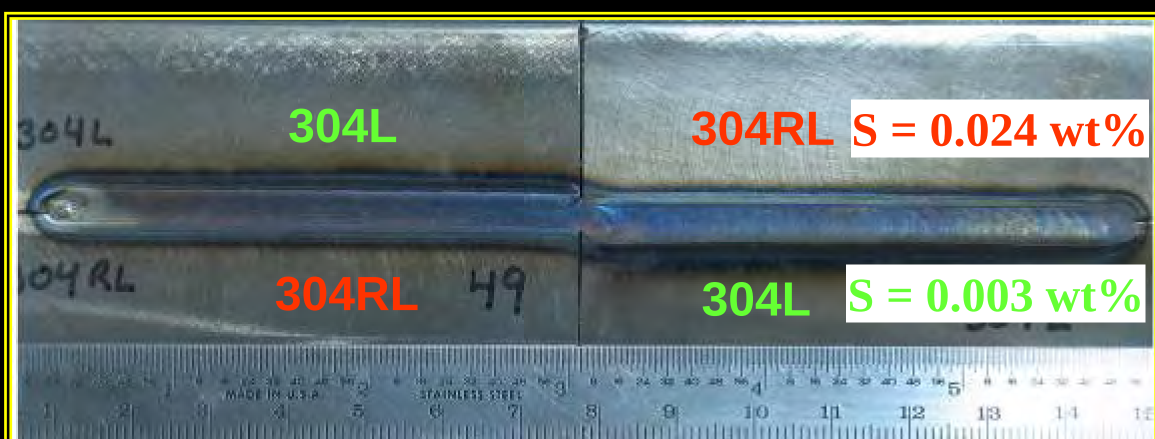

I = 101 A, V = 9.6 V, Welding speed = 1.7 mm/s

The arc shifts towards the low sulfur side

Sulfur distribution in the weld

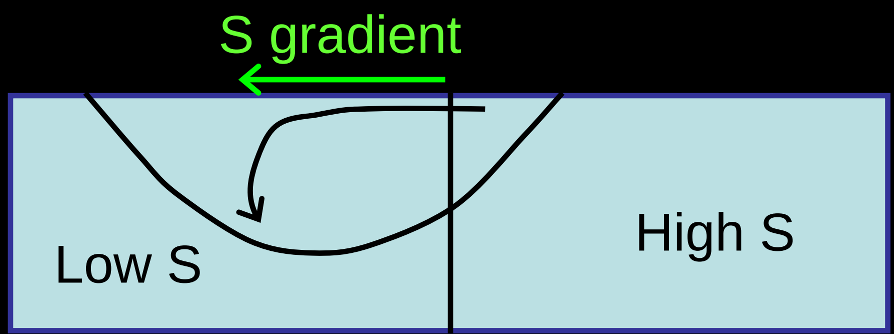

EPMA results

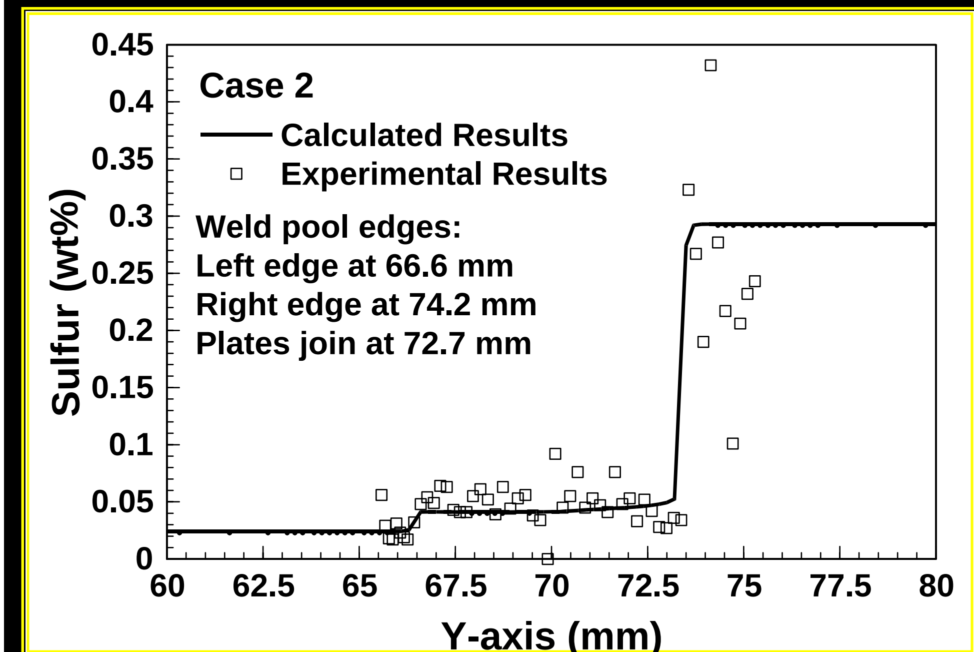

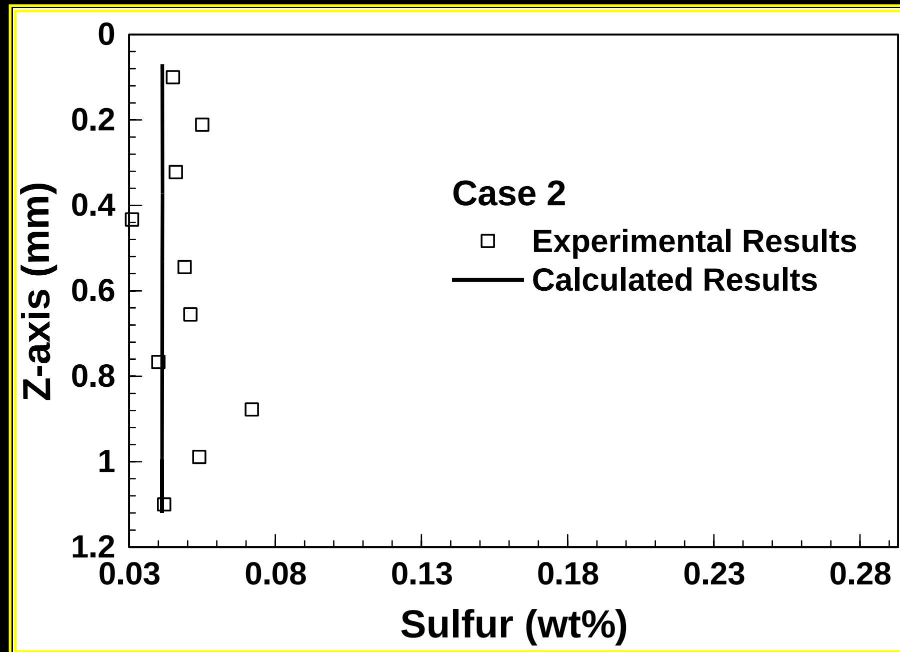

Welding conditions: 150 A, 10.8 V, welding speed is 1.7 mm/s

No significant sulfur concentration gradient
=> Not much influence on weld bead shift

Reason for arc shift

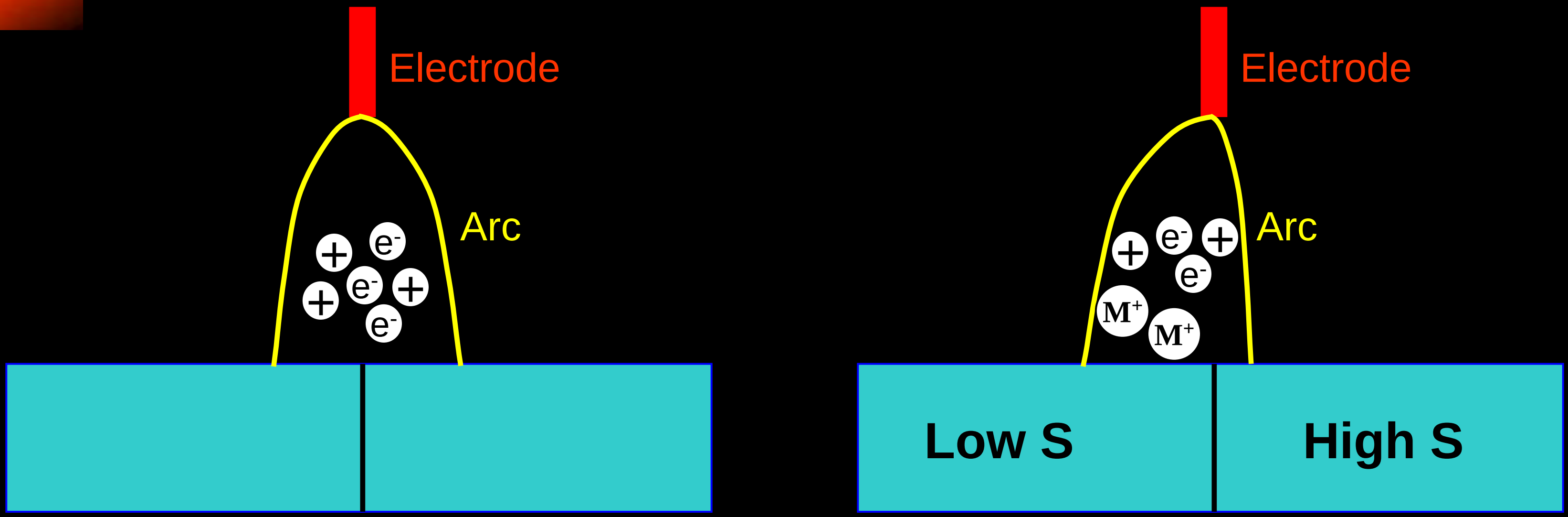

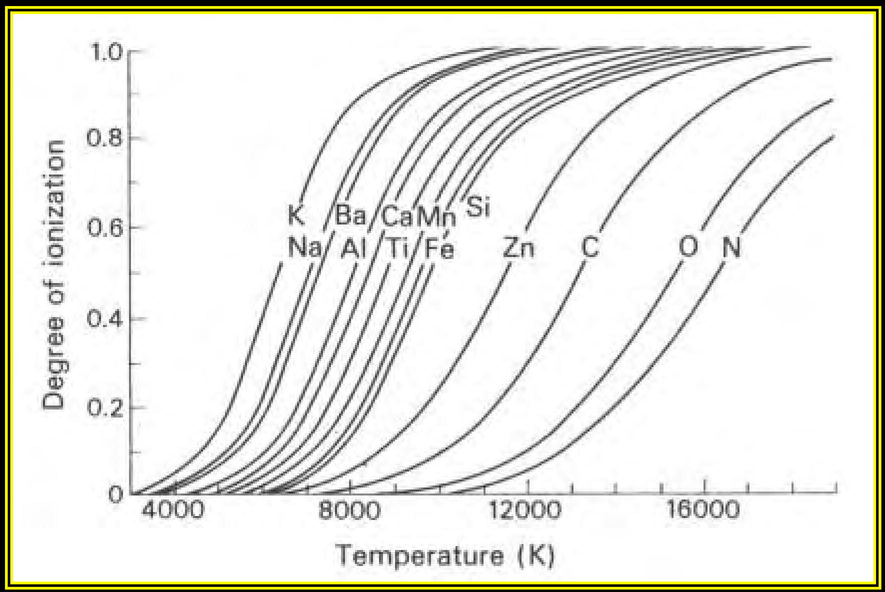

- Sulfur covers more surface on high sulfur side => less metal sites on the surface.
- Sulfur has strong interaction with low ionization potential metals like Mn. Higher the sulfur the more it prevents ionization.

Incorporating arc shift

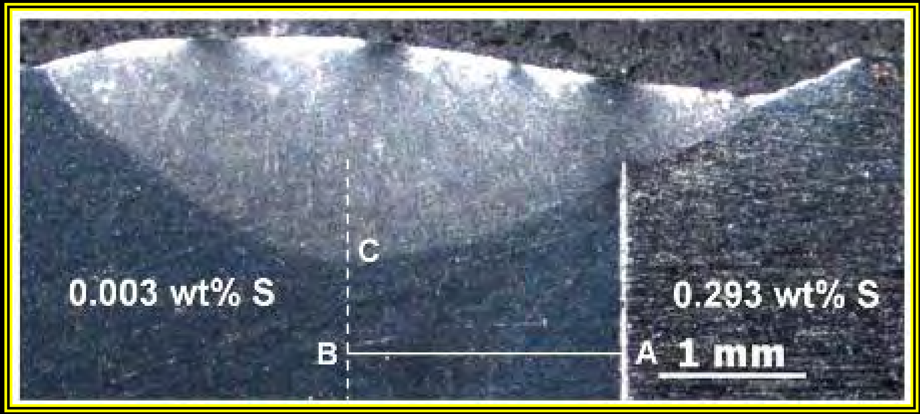

Maximum penetration occurs approximately below the arc location

Amount of arc shift is approximated by length AB

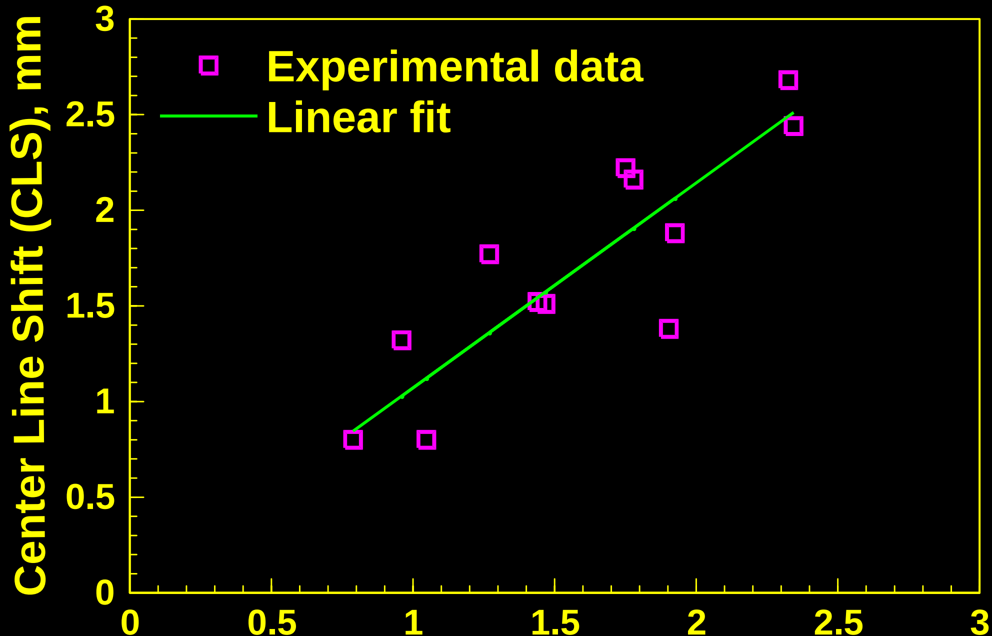

$$0.19 \times \left| C_L - C_R \right|^{0.24} \times \left(\frac{I \times V}{U} \right)^{0.42}, (\mathrm{wt\%})^{0.24} - (\mathrm{J/mm})^{0.42}$$

Empirical relation for amount of arc shift

Temperature and velocity fields & Sulfur distribution

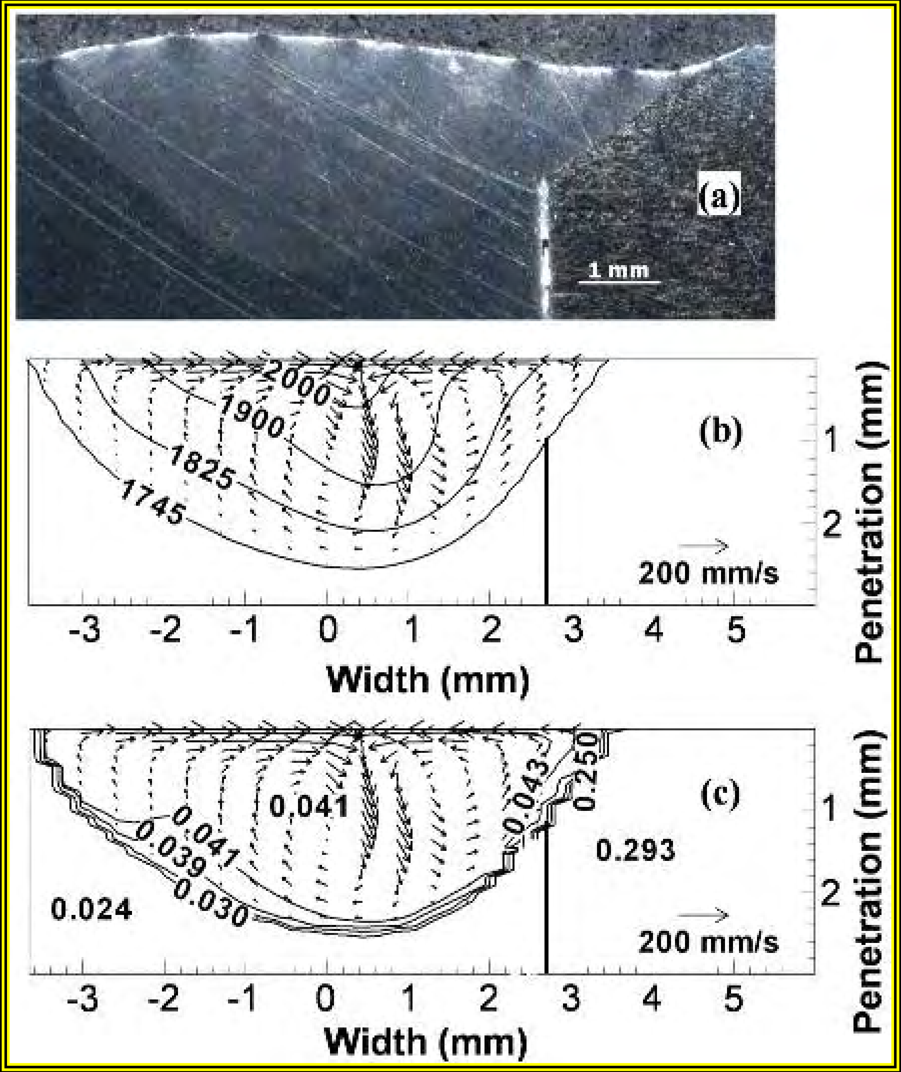

Welding conditions: 150 A, 10.8 V, welding speed is 1.7 mm/s

No significant sulfur gradient except very close to the edges

Fair agreement between the calculated and experimental weld pool geometry

5. Uphill, downhill, tilt, L and V configurations

Effect of tilt angle

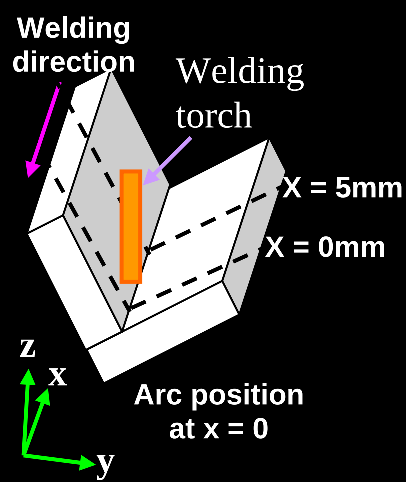

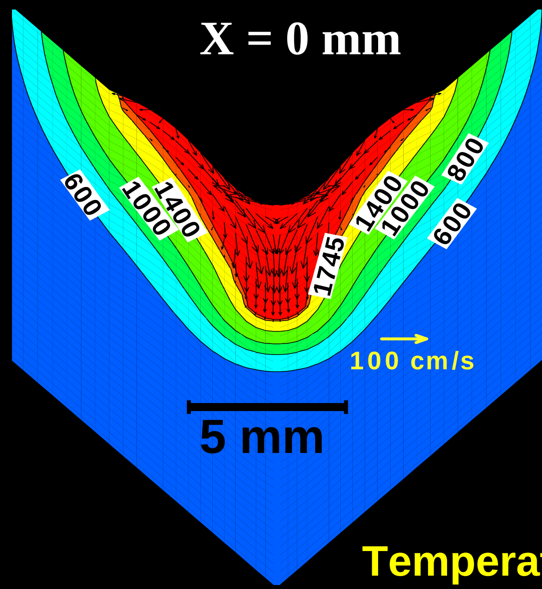

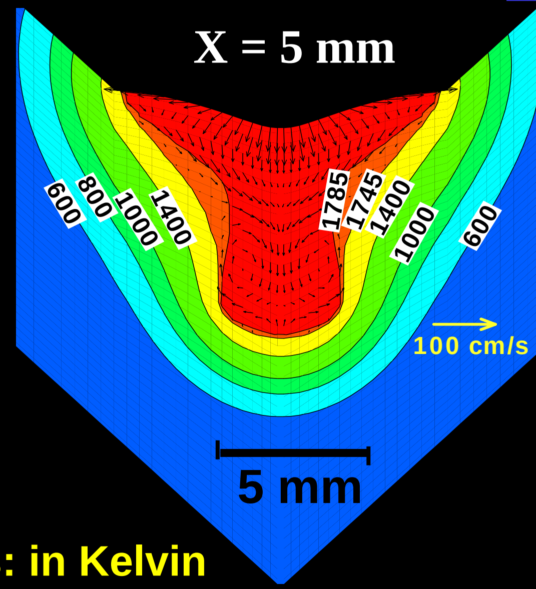

Temperatures: in Kelvin

Weld pool boundary: 1745 K

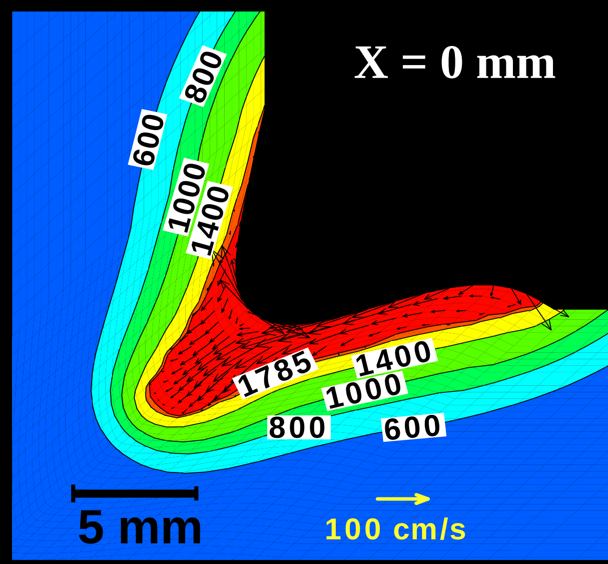

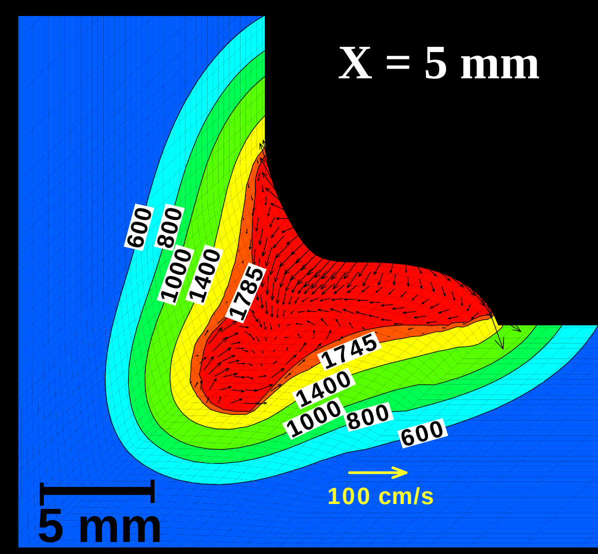

Welding Conditions

I = 362 A

V = 33 V

U_w = 4.2 mm/s

CTWD = 22.2 mm

w_f = 211.7 mm/s

$$Pe = \frac{uL}{\alpha} = 120$$

u: Liquid velocity

L: Weld pool width

α: Thermal diffusivity

Effect of lift angle

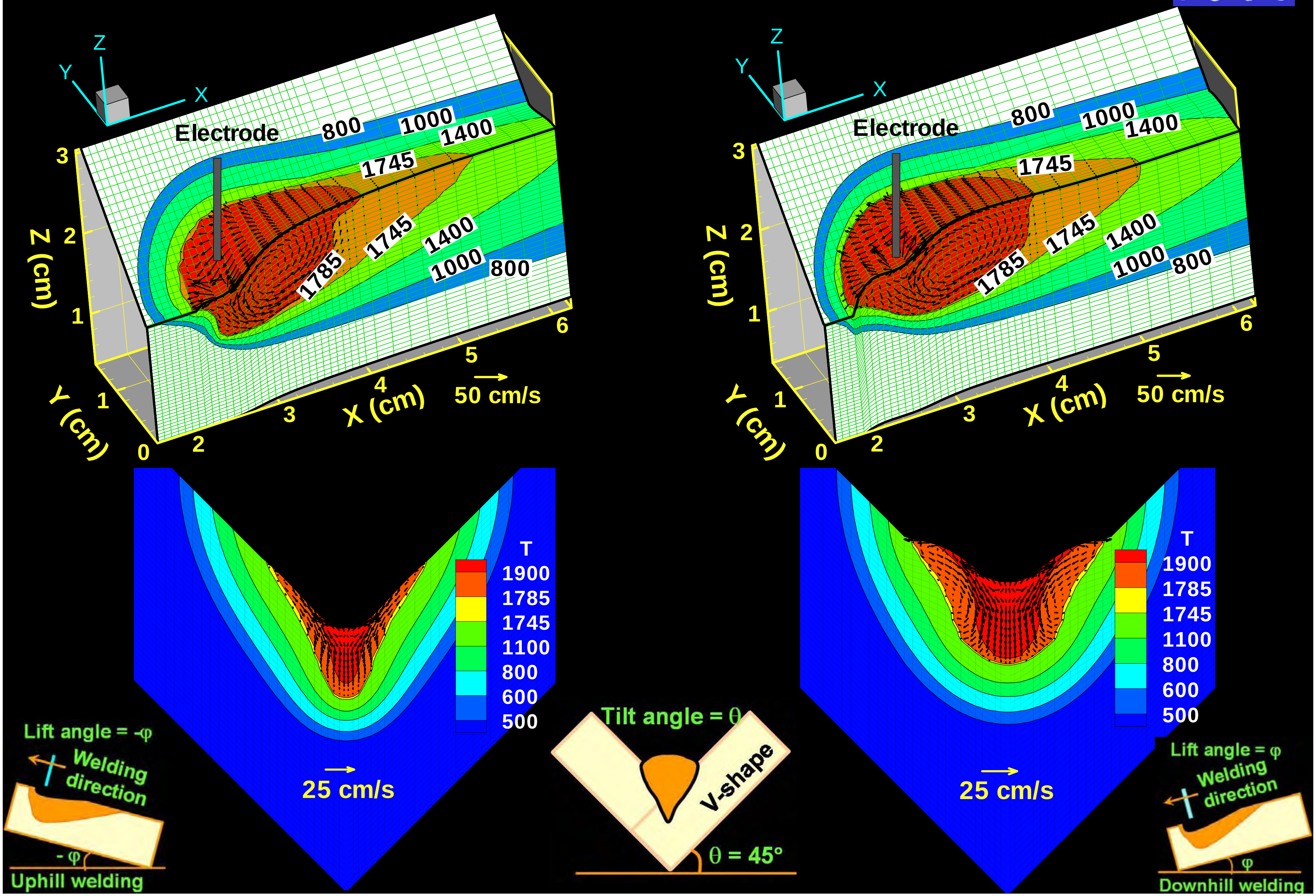

Weld bead geometry

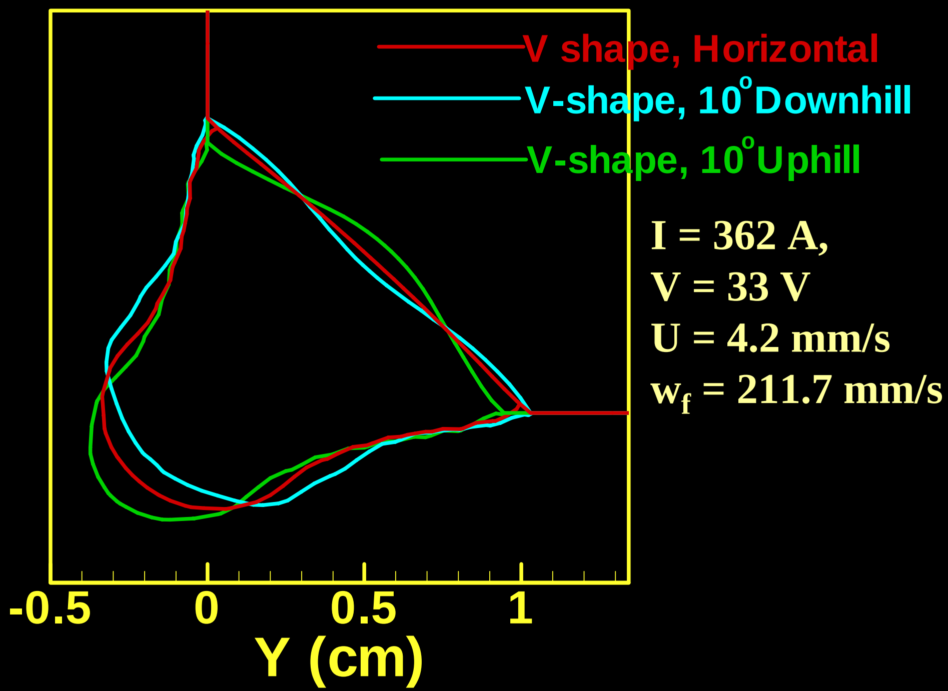

- ✪ Weld bead is depressed in the center during downhill welding
- ✪ Hump formation during uphill welding
- ✪ More penetration during uphill welding

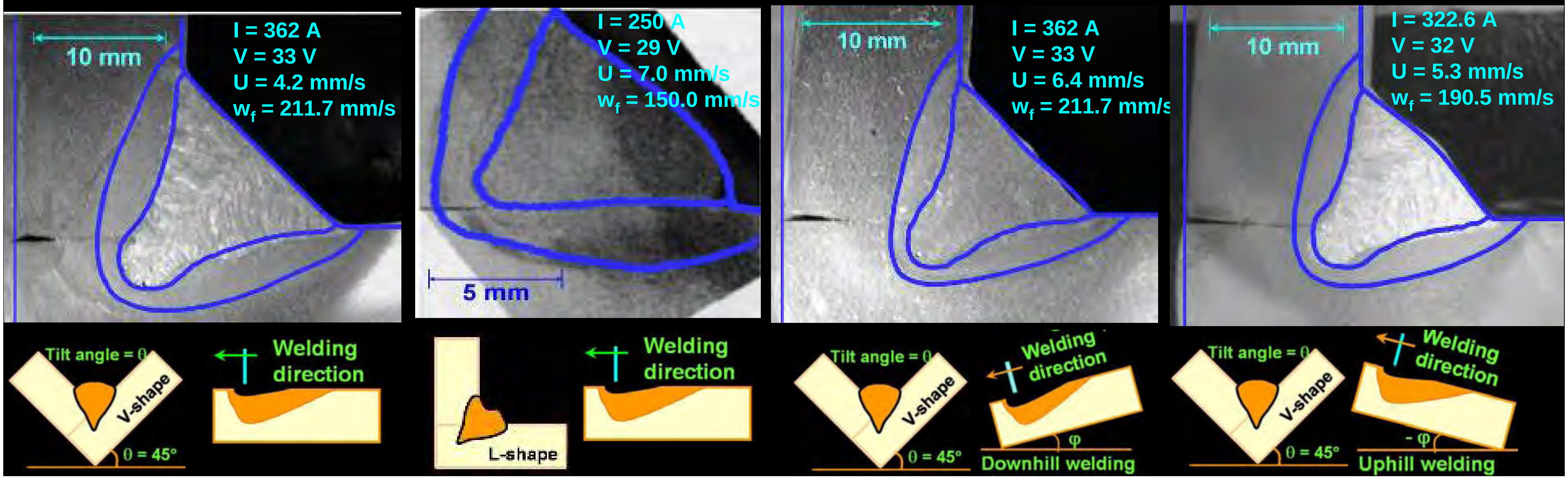

6. Composition change

Pronounced weld metal composition change

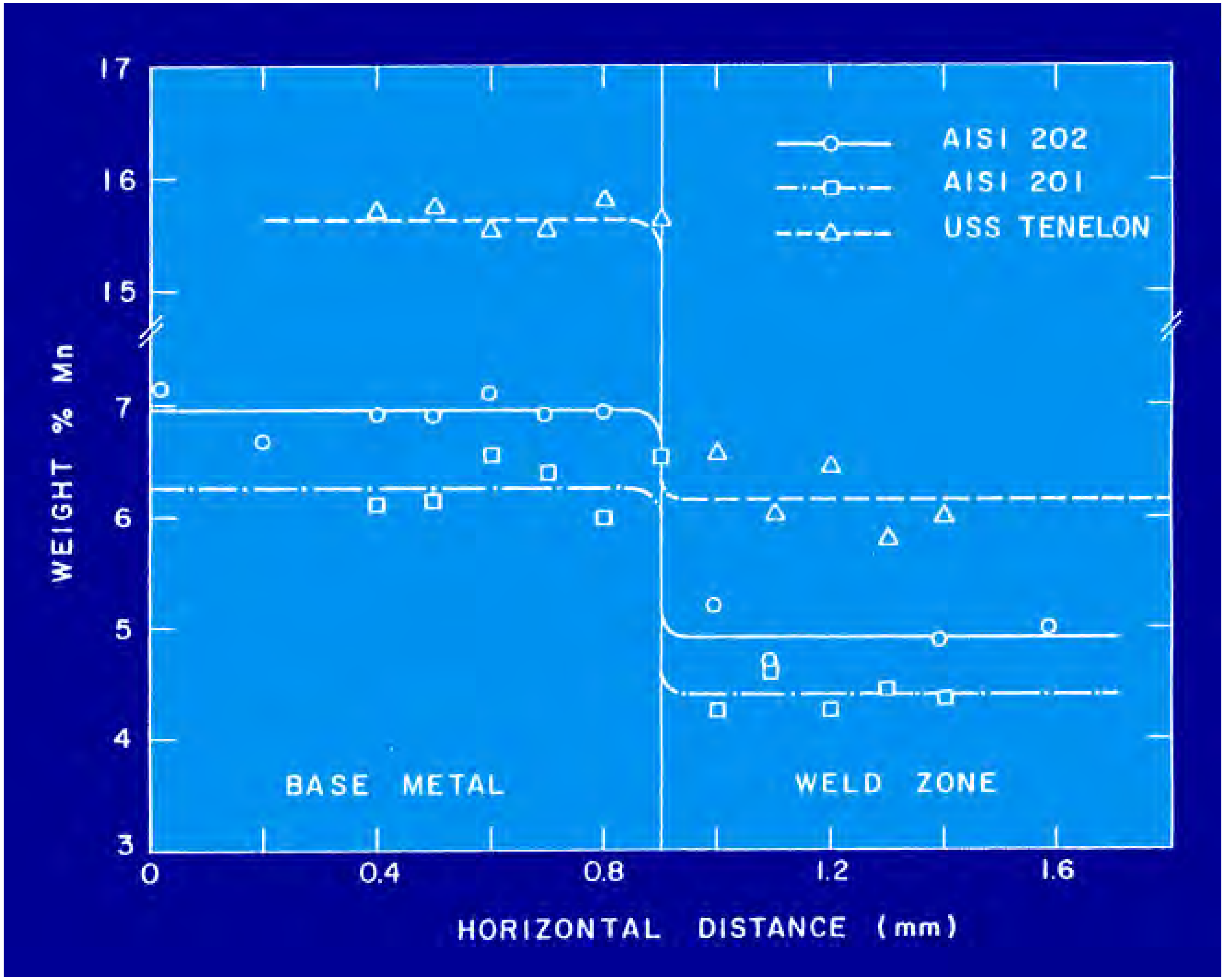

Temperature field and weld pool size are important factors

Composition change is more pronounced at low powers – why?

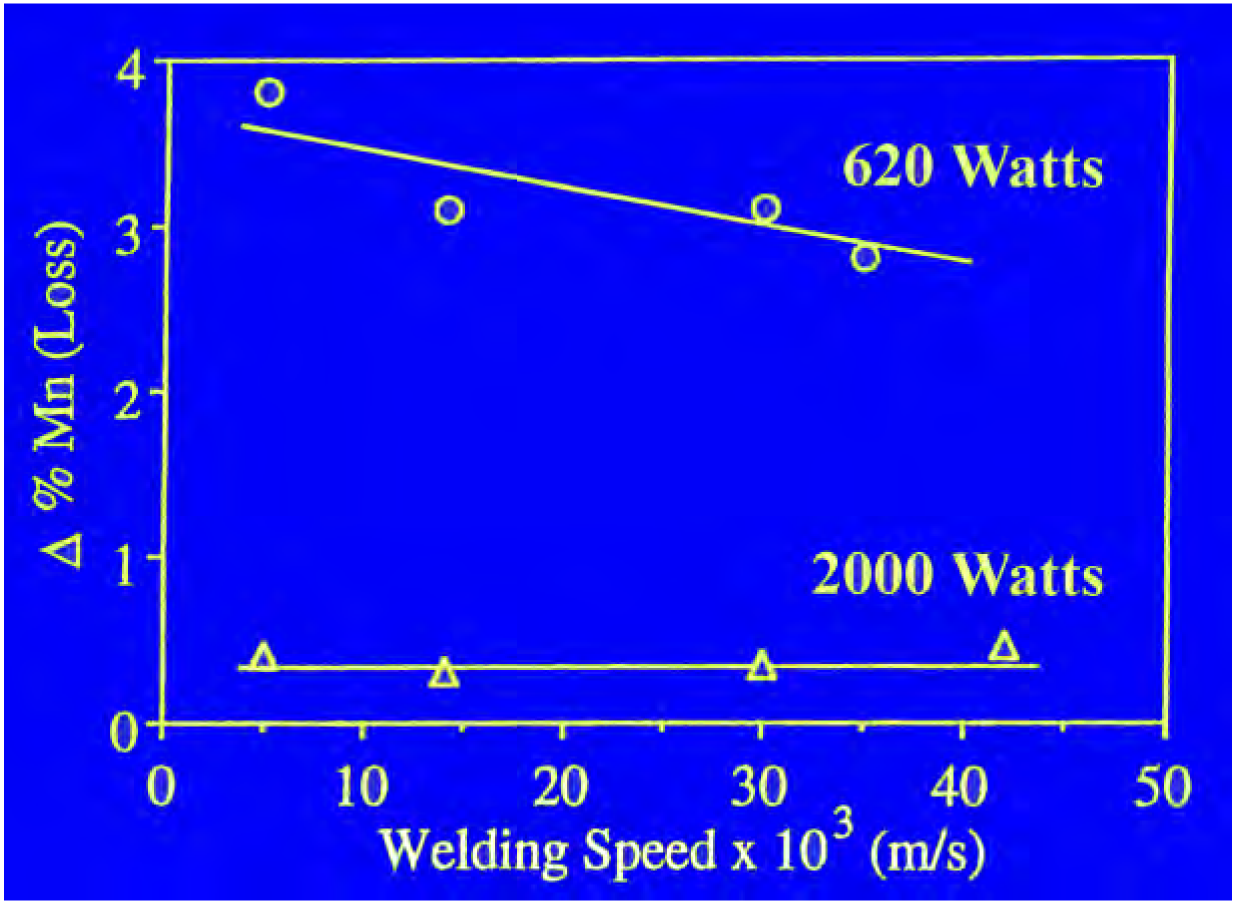

Why is the composition change more pronounced at low powers?

Low Power Welding

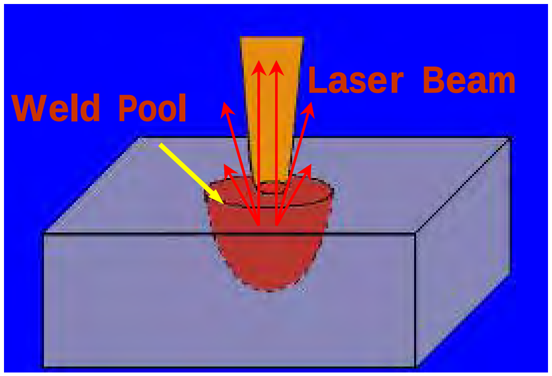

Base Metal

High Power Welding

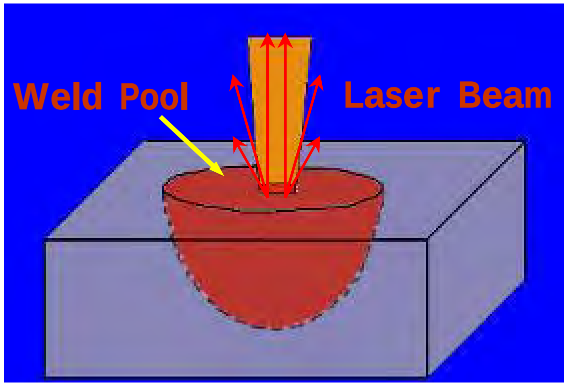

Base Metal

- Most of the evaporation takes place under the beam
- Pool size increases strongly with increase in power – alloying element loss is spread over a larger volume

Temperature from Vapor Composition

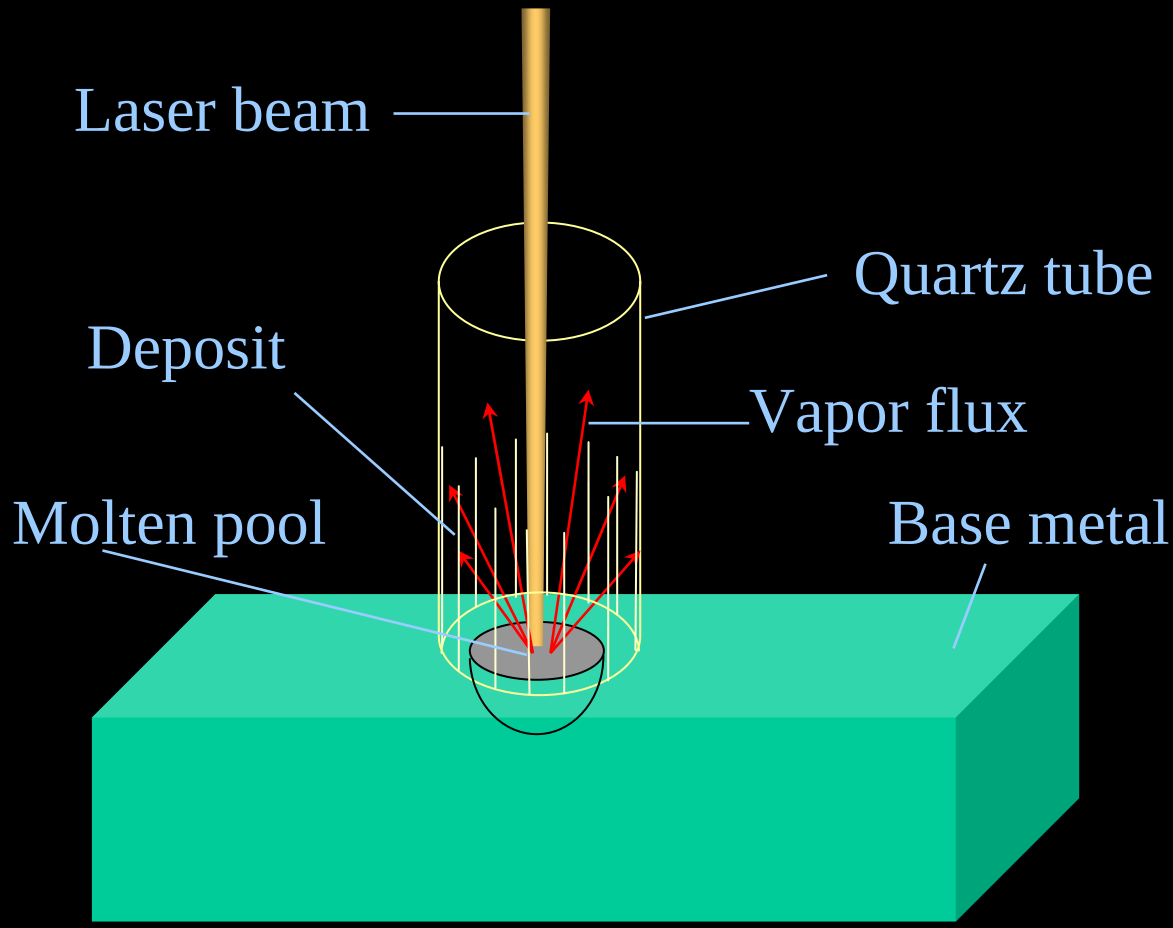

$$\frac{\text{Vaporization rate of A}}{\text{Vaporization rate of B}} = \frac{J_A}{J_B} = \frac{p_A}{p_B}\sqrt{(M_B/M_A)} = f\,(T)$$

Temperature from Vapor Composition

$$\frac{\text{Vaporization rate of A}}{\text{Vaporization rate of B}} = \frac{J_A}{J_B} = \frac{p_A}{p_B}\sqrt{(M_B/M_A)}$$

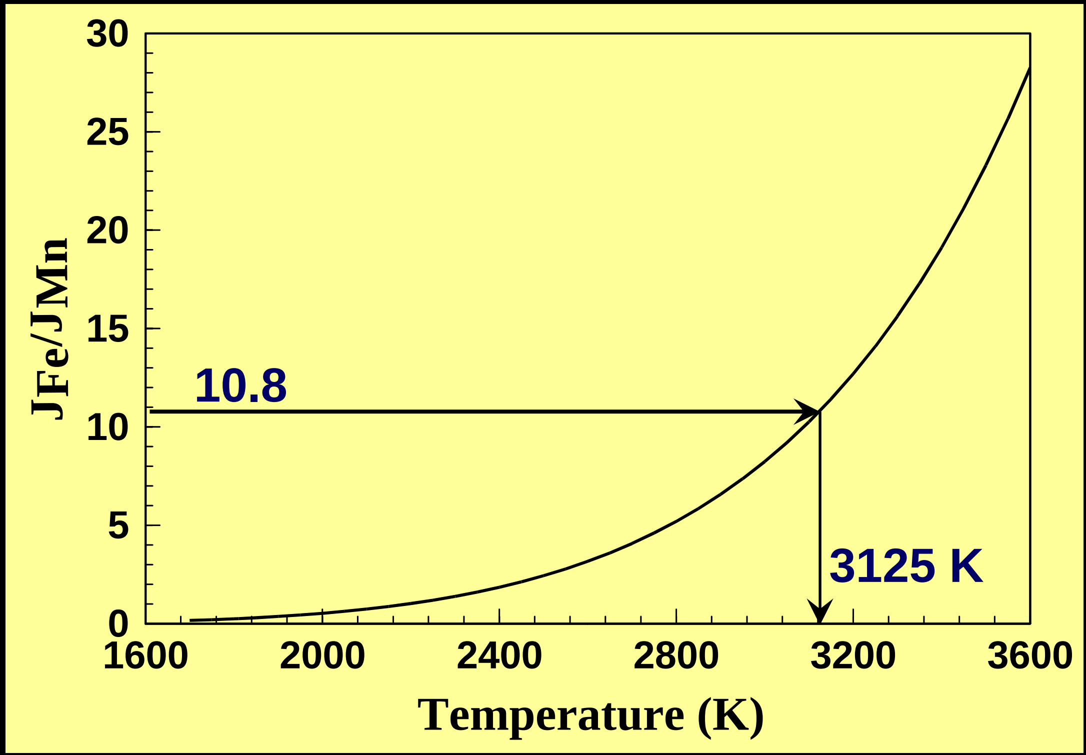

Temperature from Vapor Composition

Power and pulse	Spot radius (mm)	Peak temperature from numerical heat transfer (K)	Temperature from J_{Fe}/J_{Mn} (K)	Temperature from J_{Cr}/J_{Mn} (K)
1067 W, 3.0 ms pulse	0.260	3270	3125	3110
	0.325	2879	3005	2865
530 W, 4.0 ms pulse	0.210	2761	3090	3060
	0.313	2308	2435	2485

Model Validation

Experimental and Calculated Weld Pool Cross Sections

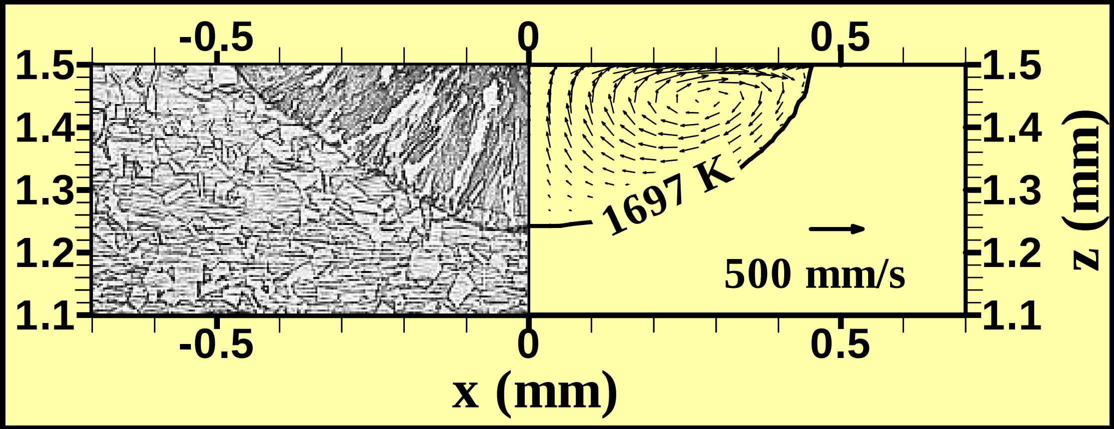

(a) beam radius: 0.43 mm

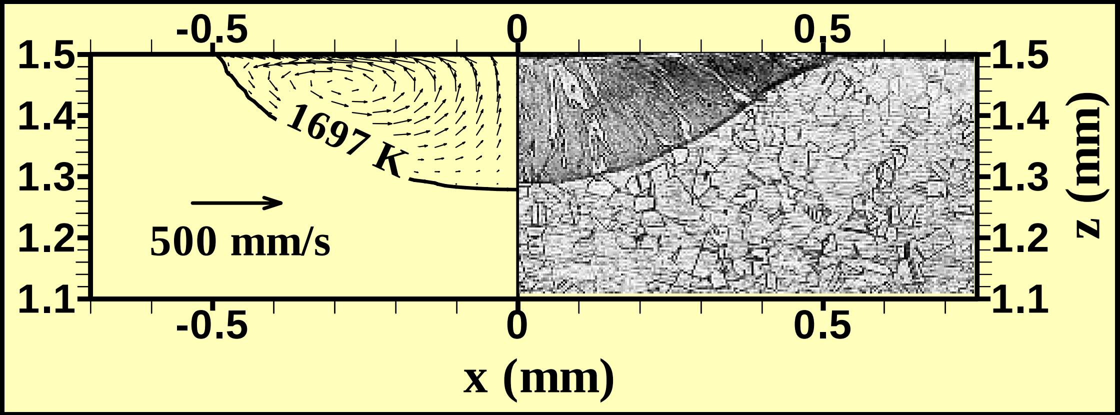

(b) beam radius: 0.57 mm

Laser power: 1967 W and pulse duration: 3 ms.

Main Metallic Species in the Vapor

Iron and chromium were the dominant species in the vapor

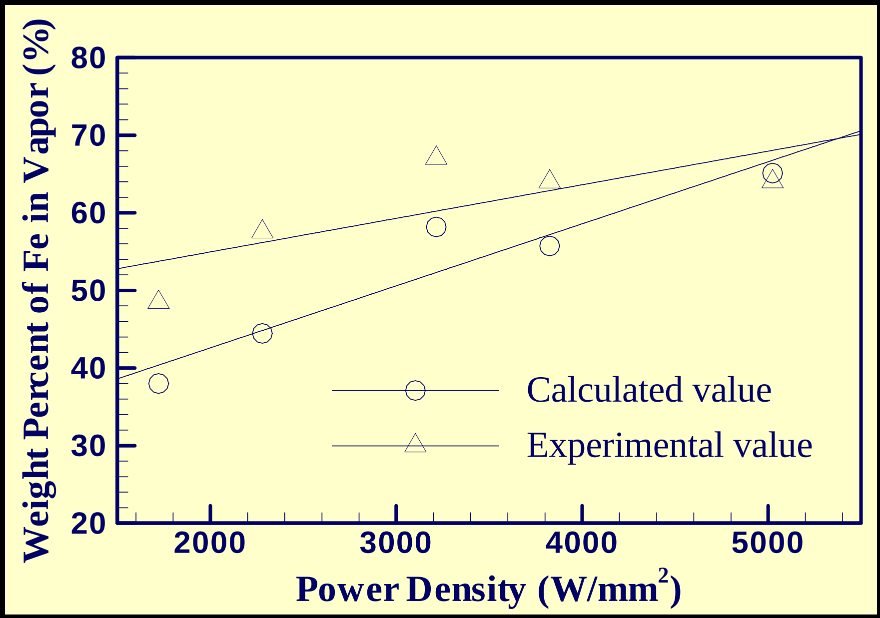

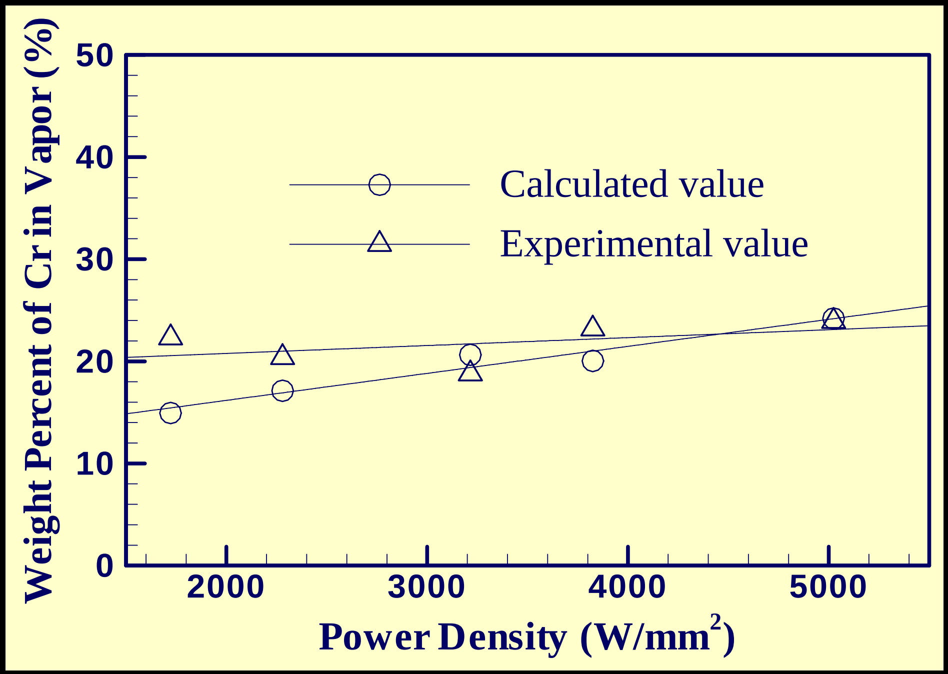

Weld Metal Composition Change

Initial concentrations:

Mn: 1 wt% , Cr: 18.1 wt%,

Ni: 8.6 wt%, Fe: 72.3 wt%

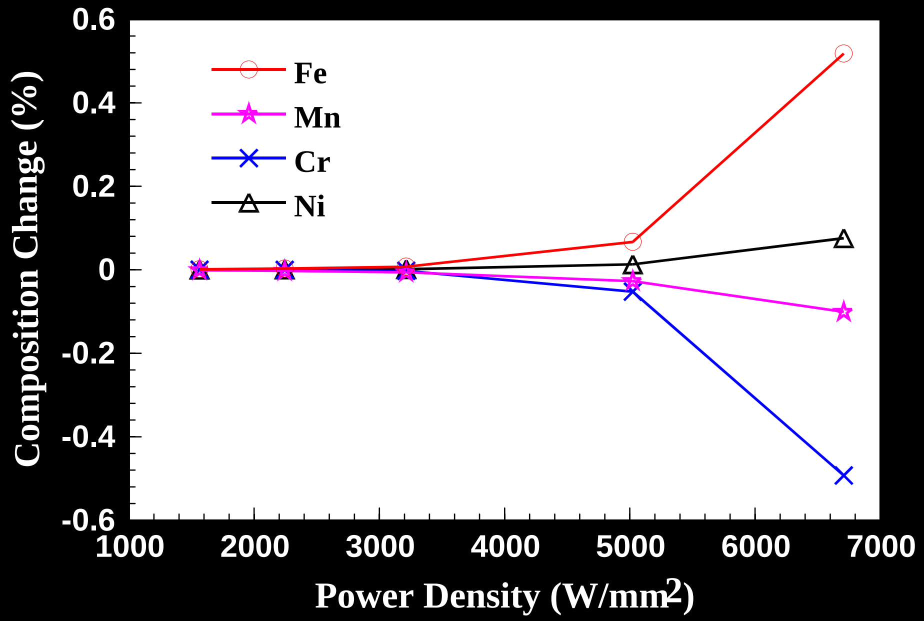

Final weight percent of element i:

$$(\%\ \ i) = \frac{V\rho(\%\ i)^{o} - \Delta m_i}{V\rho - \sum_{i=1}^{n} \Delta m_i} \times 100\%$$

V: volume of weld pool

ρ: density of liquid metal

Δm_i: weight loss of element i

n: number of vapor species

Assumption: uniform weld pool composition resulting from strong recirculating flow

Change of Composition of Weld Pool

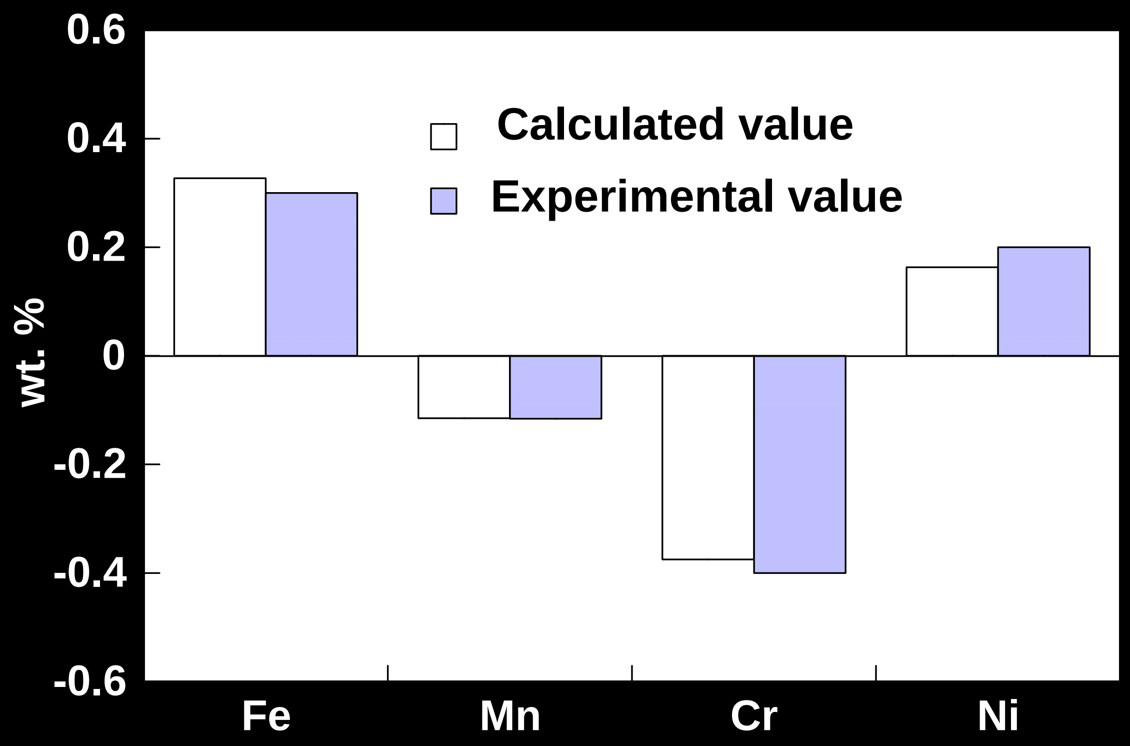

Laser power: 1067 W, pulse duration: 3.0 ms, and beam radius: 0.225 mm.

Composition Change of Weld Pool

Microprobe trace

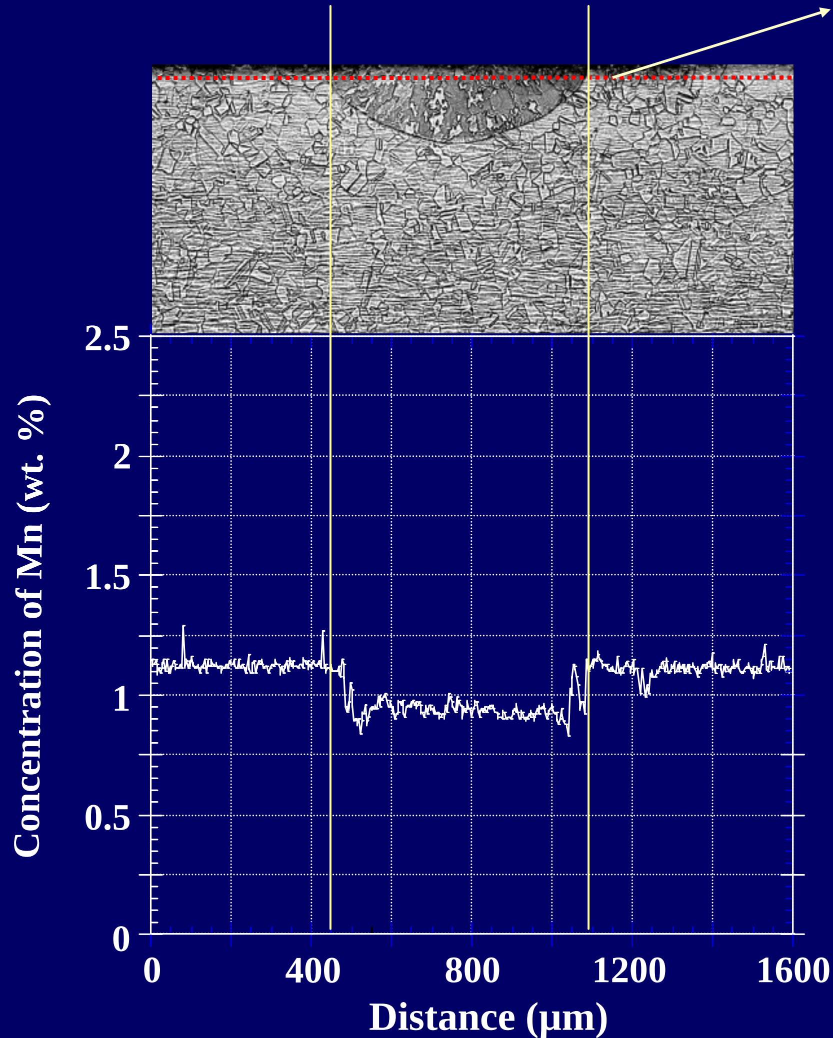

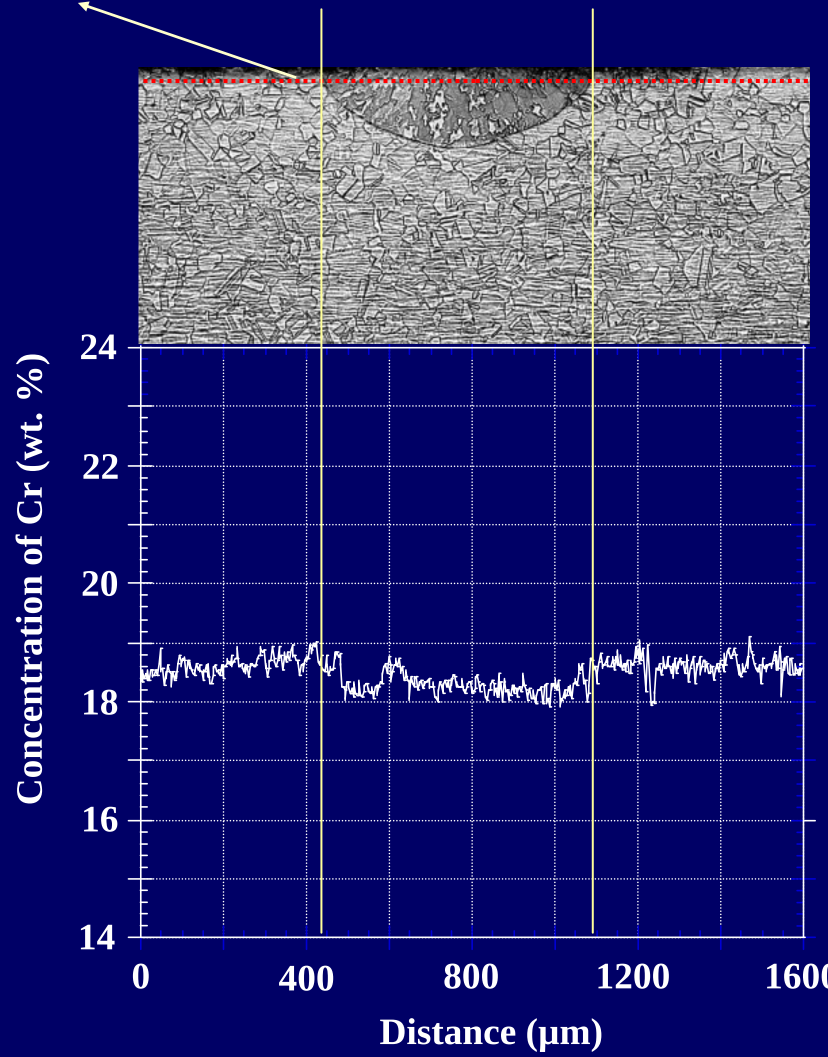

Laser power: 1067 W, pulse duration: 3.0 ms, and beam radius: 0.325 mm

Recoil and Surface Tension Forces

Laser power: 1067 W, pulse duration: 3.0 ms, and beam diameter: 0.405 mm.

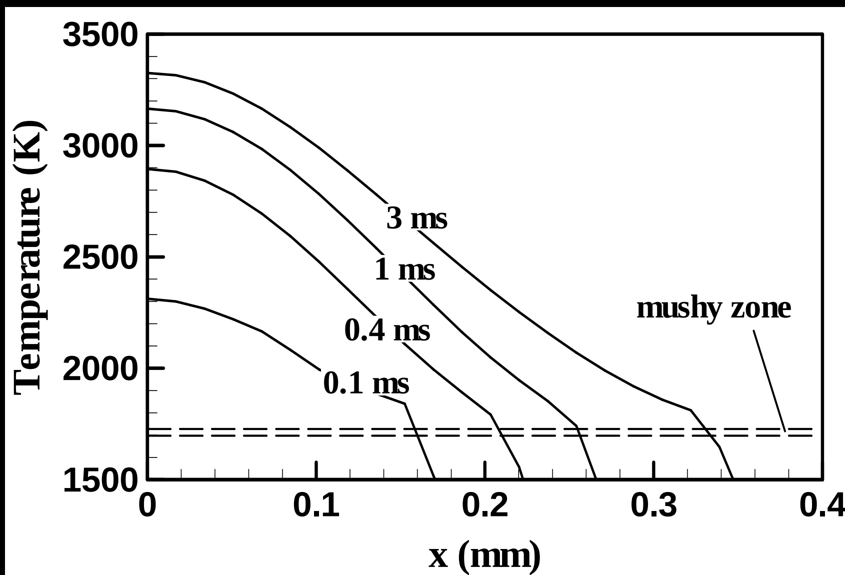

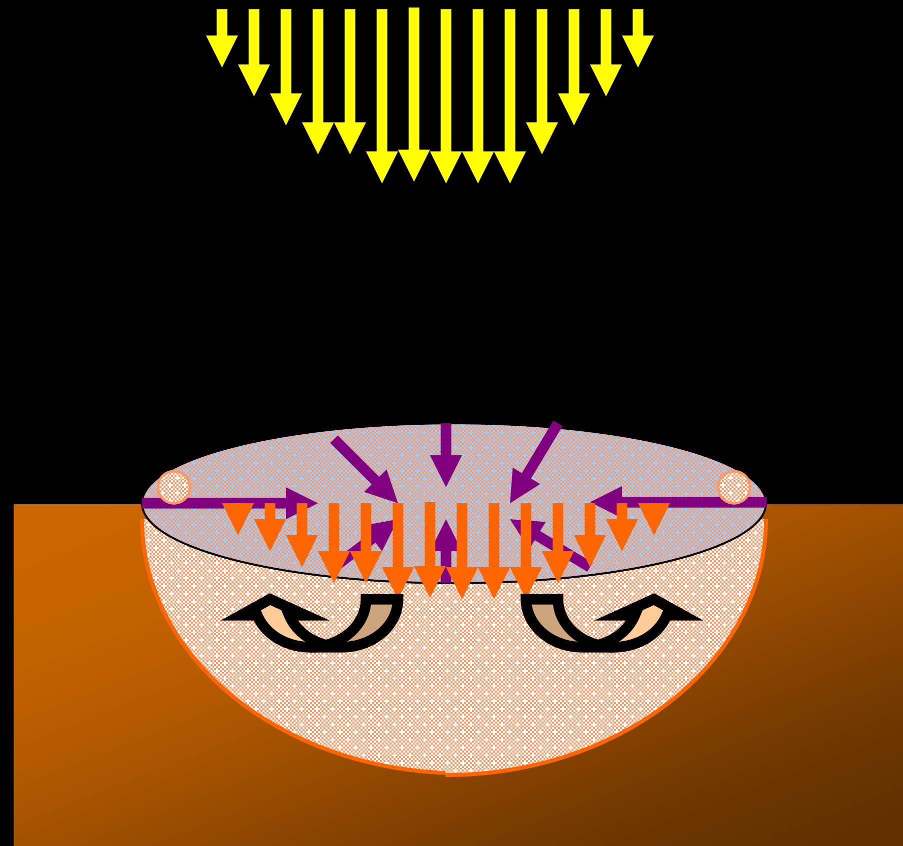

Surface tension force: $F_s = 2\pi r_0 \sigma$

Recoil force: $F_r = 2\pi \int_0^{r_B} r \Delta P(r) dr$

Recoil force > Surface tension force => Expulsion of metal drops

Recoil and Surface Tension Forces

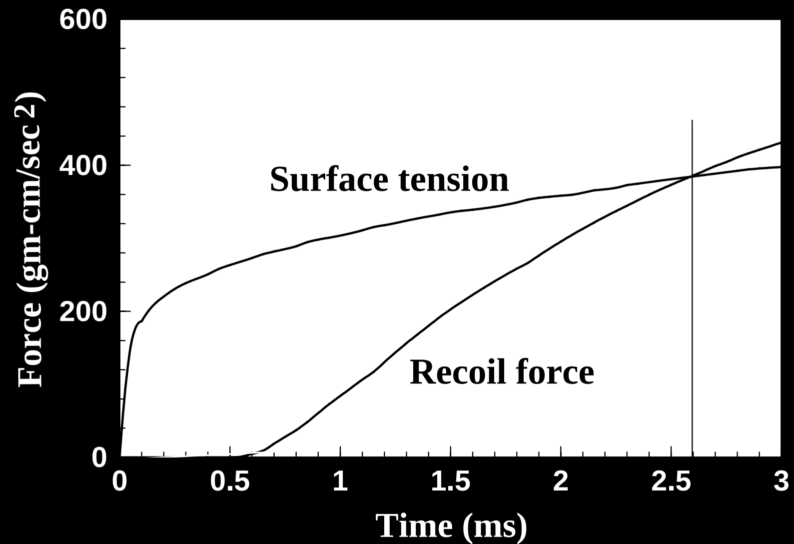

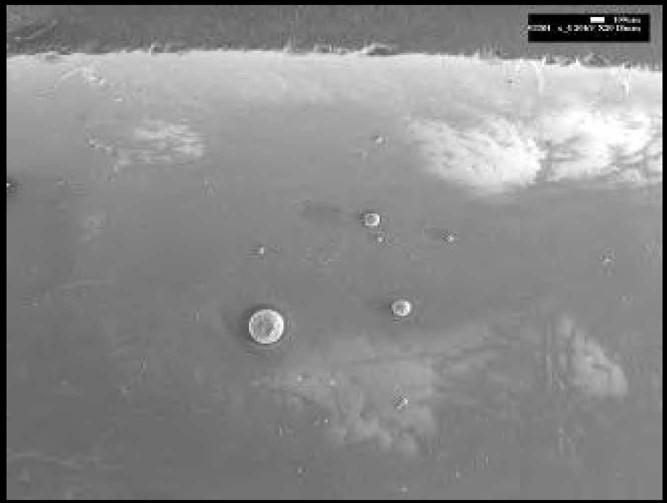

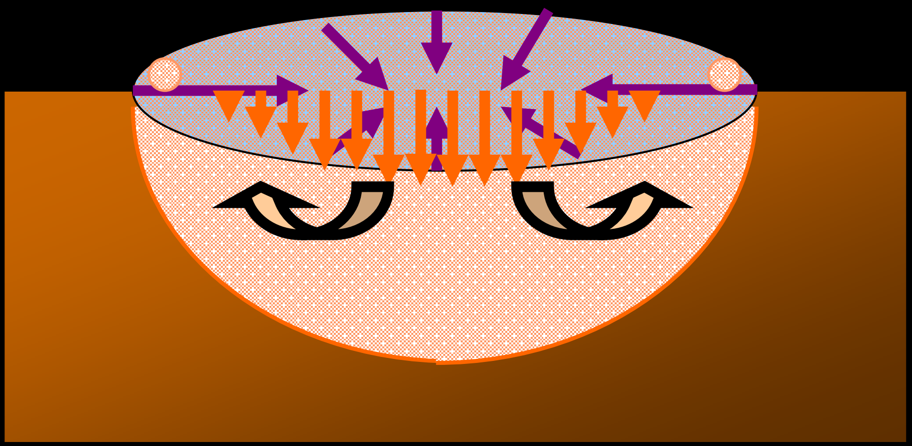

t > 2.6 ms, Recoil force > Surface tension force => Expulsion of metal drops

Free Surface Deformation

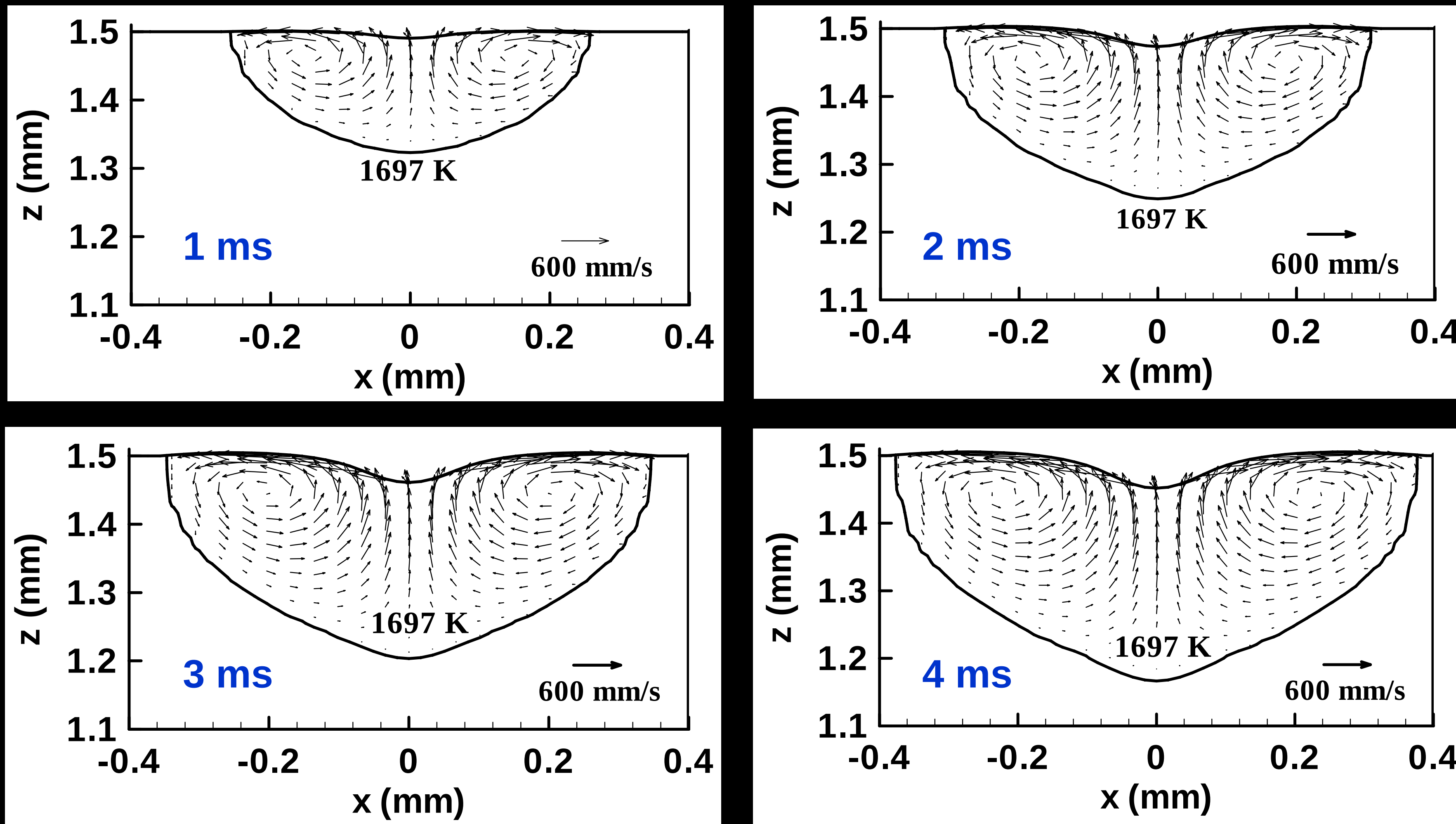

Progressive deformation of the free surface

Free Surface Deformation

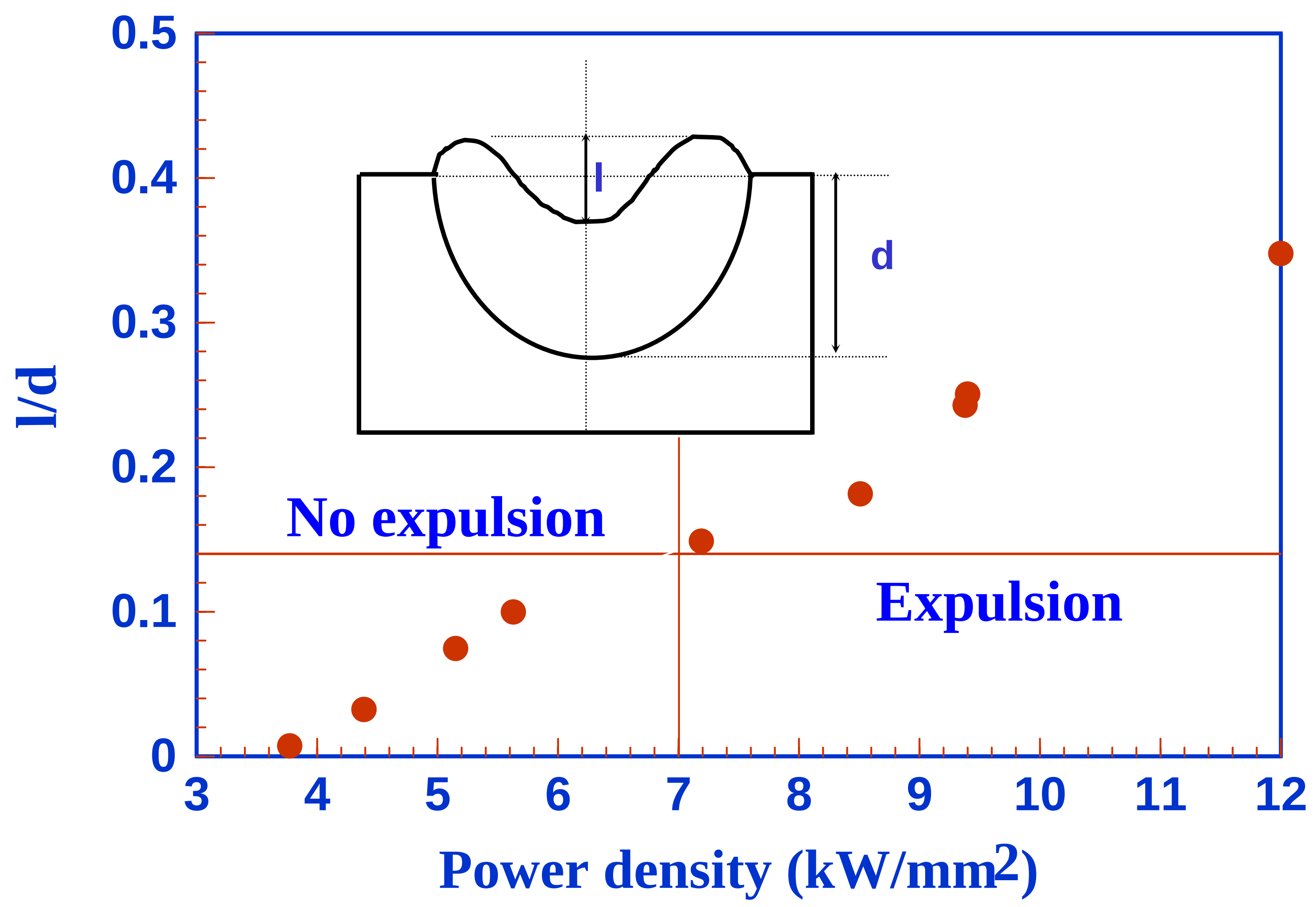

Critical Laser Power Density

3.0 ms pulse

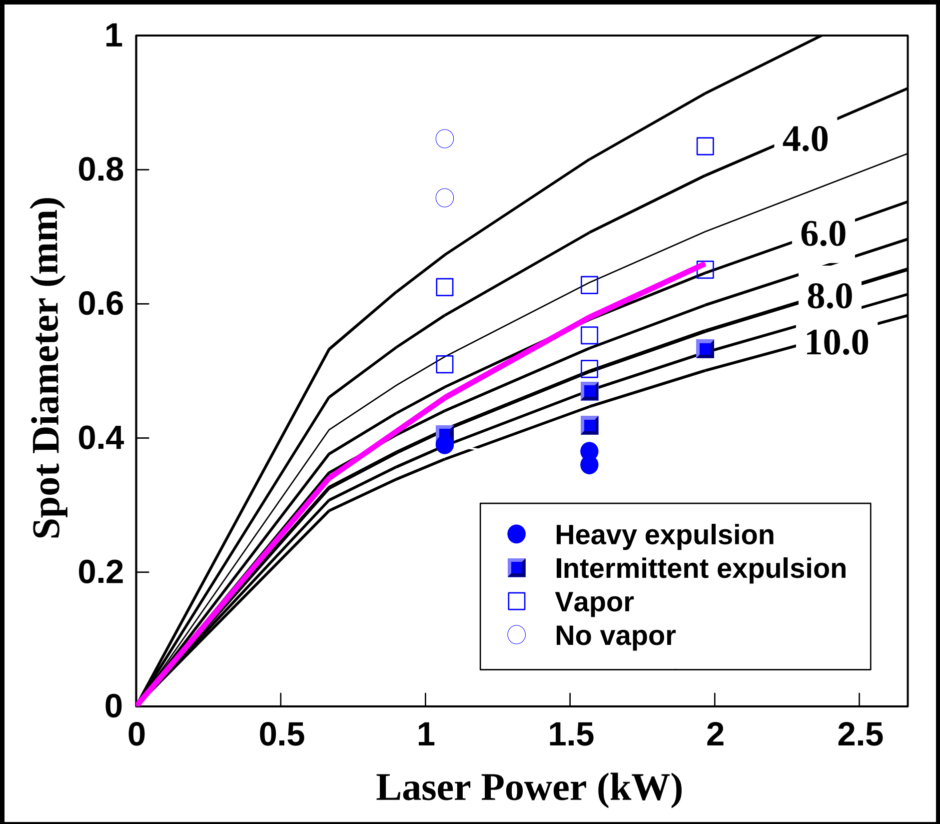

Critical laser power density:

8.0 kW/mm^2

4.0 ms pulse

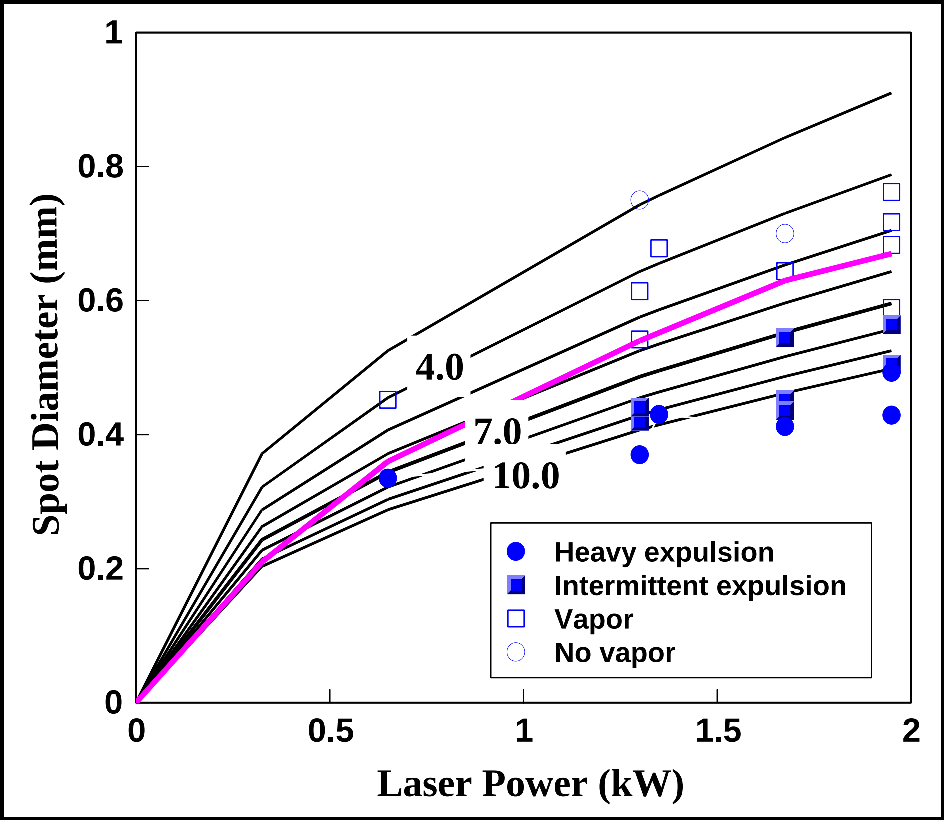

Critical laser power density:

7.0 kW/mm^2

Effects of Welding Variables

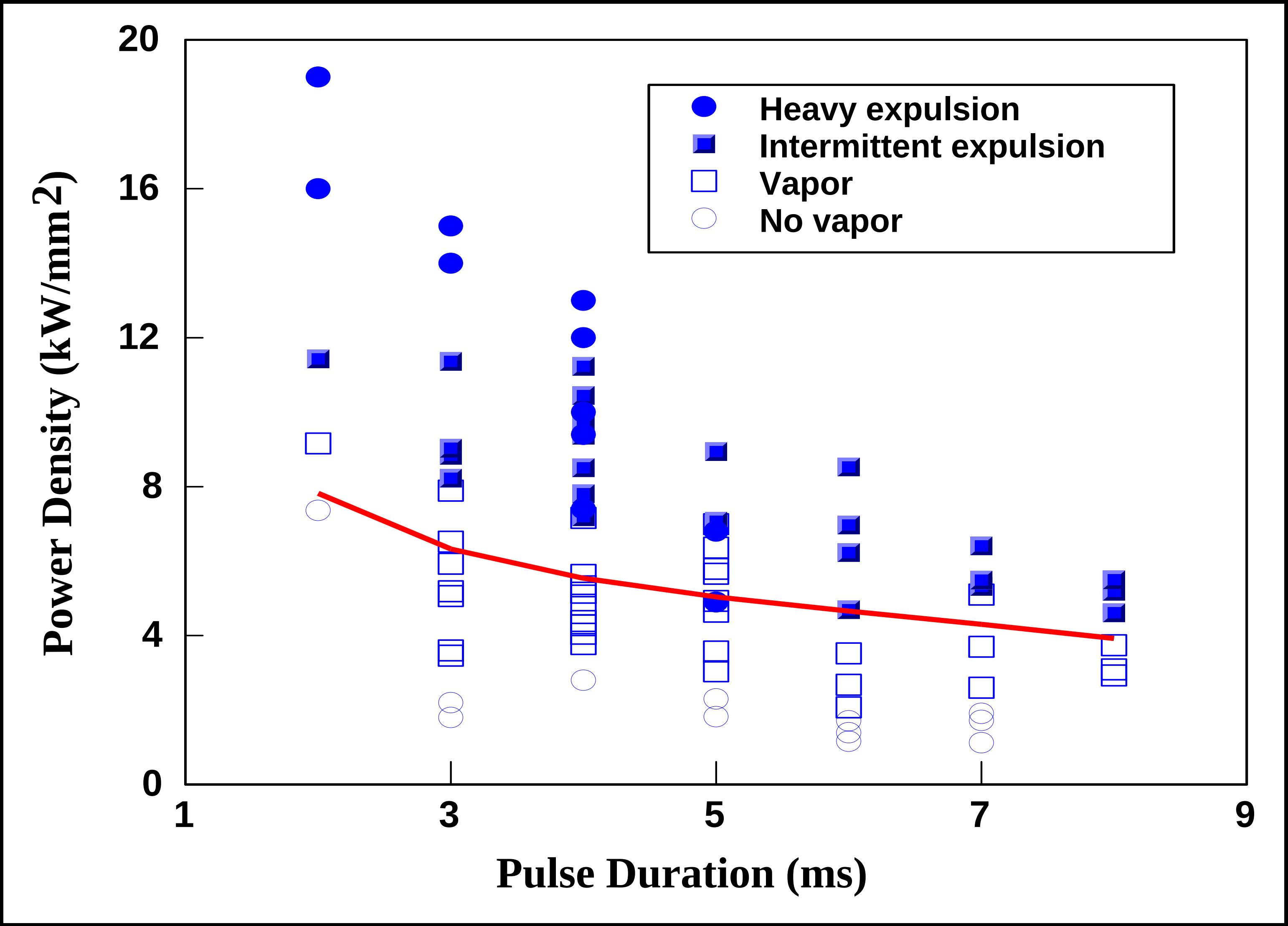

7. Dissolution of gases

Nitrogen Dissolution In The Weld Pool

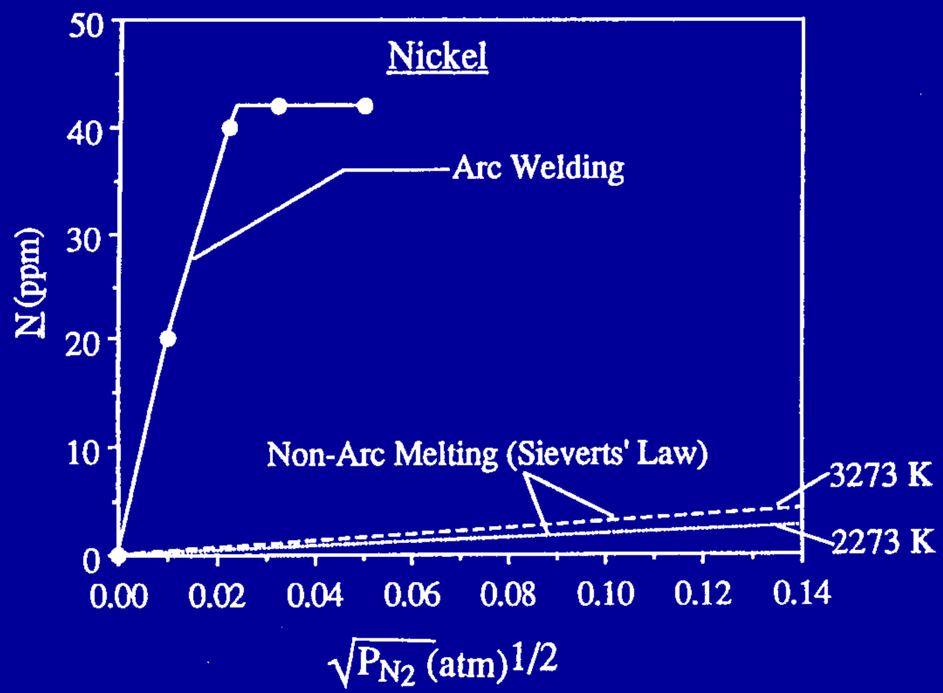

Nitrogen concentration in the weld metal is much higher than that predicted by Sieverts' law

But why?

Nitrogen dissolution from a plasma environment

SYSTEM	GAS/METAL	PLASMA/METAL
SPECIES	N_2/Fe	$N_2, N_2^*, N_2^+, N, N^*$/Fe
LAW	SIEVERTS' LAW	??

SYSTEM	GAS/METAL	PLASMA/METAL
Source of N Gas	Thermal Dissociation	Thermal Dissociation Electron Impact Electromagnetic Effects
Partial Pressure	$\frac{1}{2} N_2(g) \rightarrow N(g)$ $P_N = K_{eq}^{T_s} P_{N_2}^{1/2}$	$P_N > K_{eq}^{T_s} P_{N_2}^{1/2}$ $P_N = K_{eq}^{T_d} P_{N_2}^{1/2}$

T_s = Sample Temperature T_d = Temperature at which N_2(g) dissociates

Nitrogen - Iron System

DIATOMIC NITROGEN

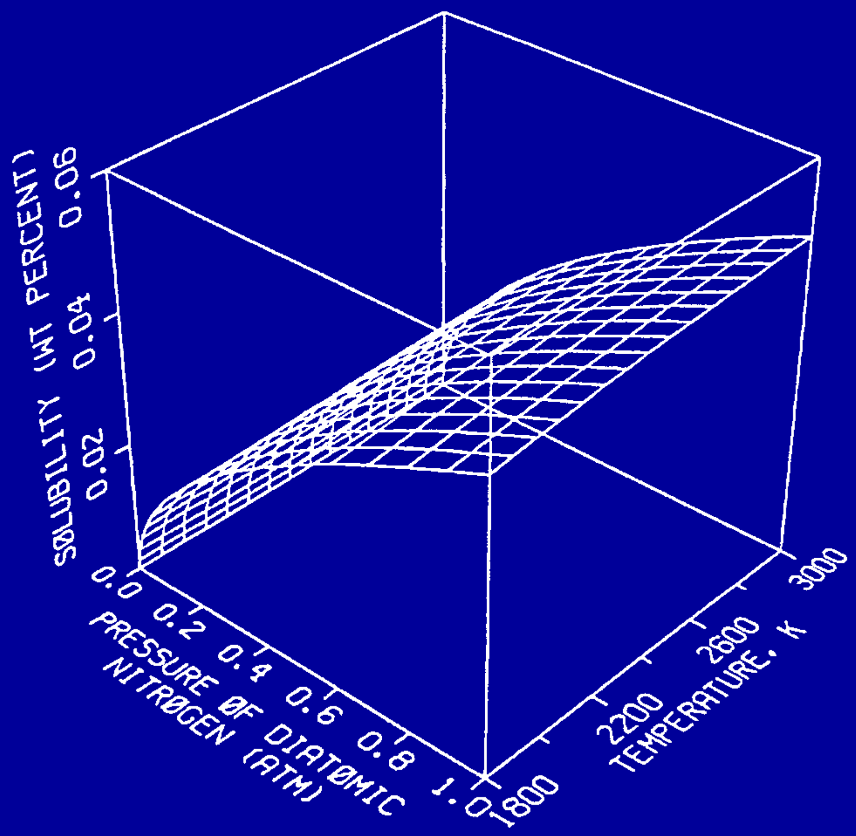

MONATOMIC NITROGEN

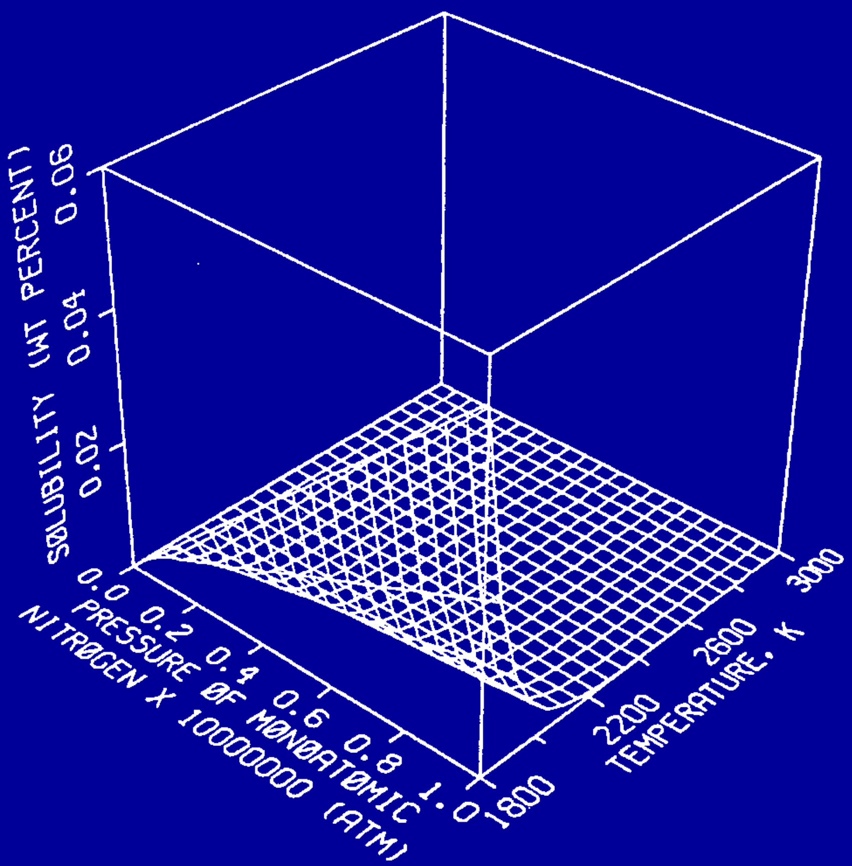

Physical modeling with isothermal metal drops

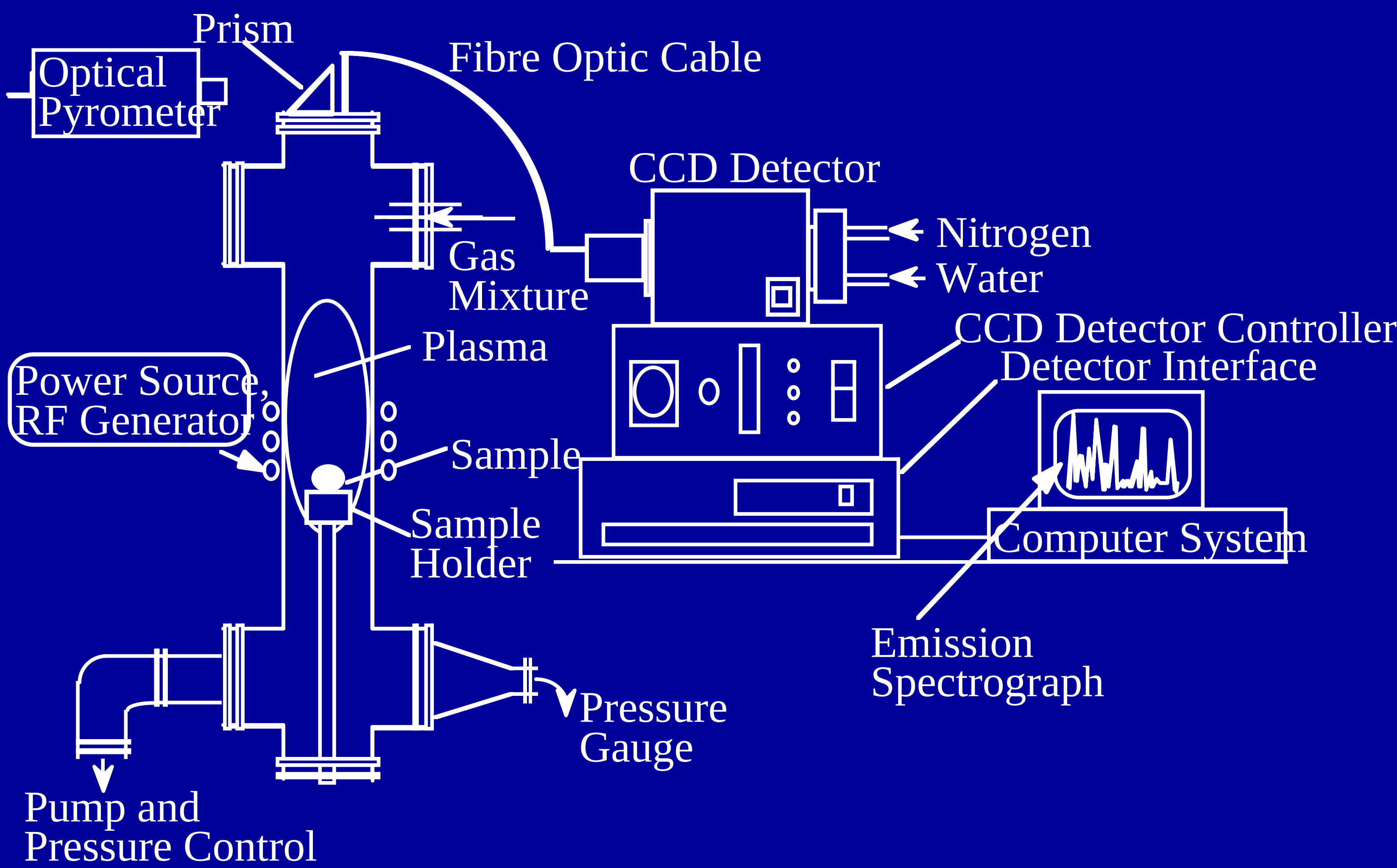

Enhanced dissolution of nitrogen in isothermal metal drops

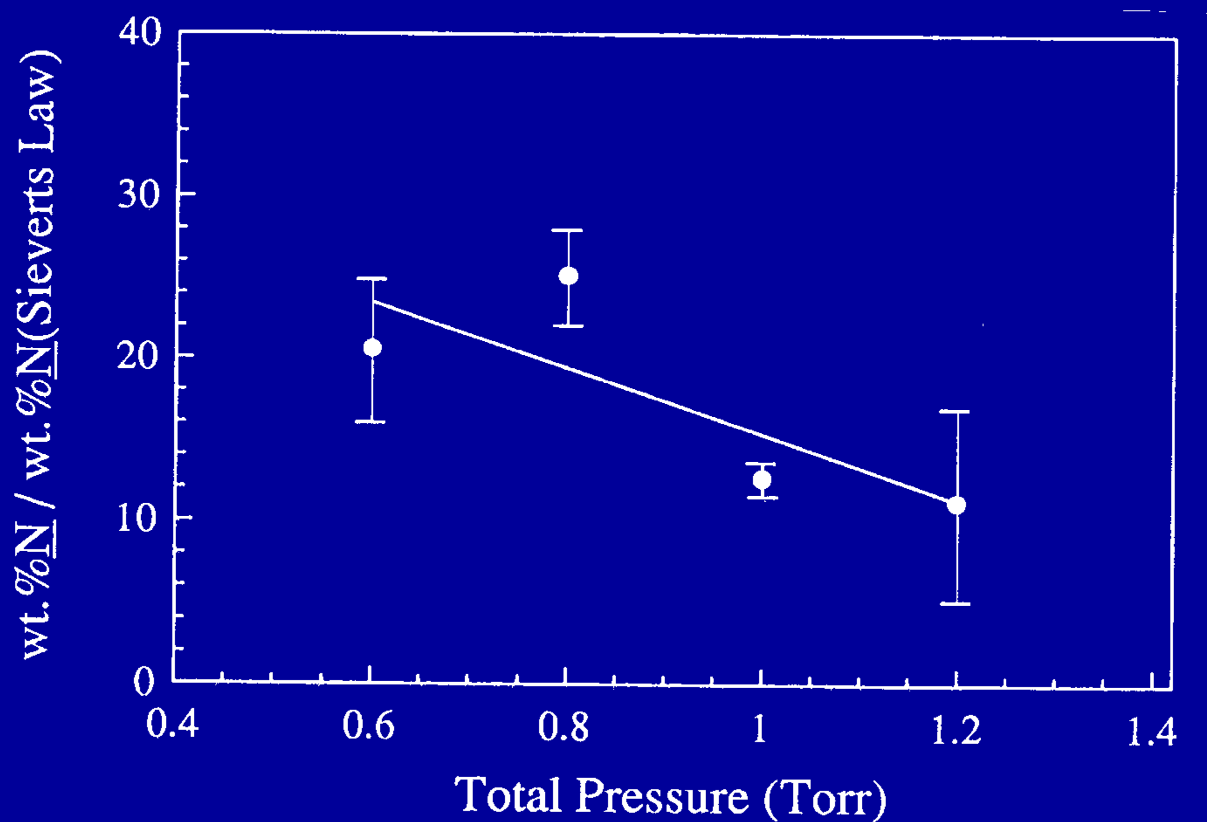

- **Nitrogen solubilities up to 30 times larger than Sieverts' Law predictions.**
- **Small changes in sample temperature cause large variations in N.**

Emission spectroscopy of glow discharges

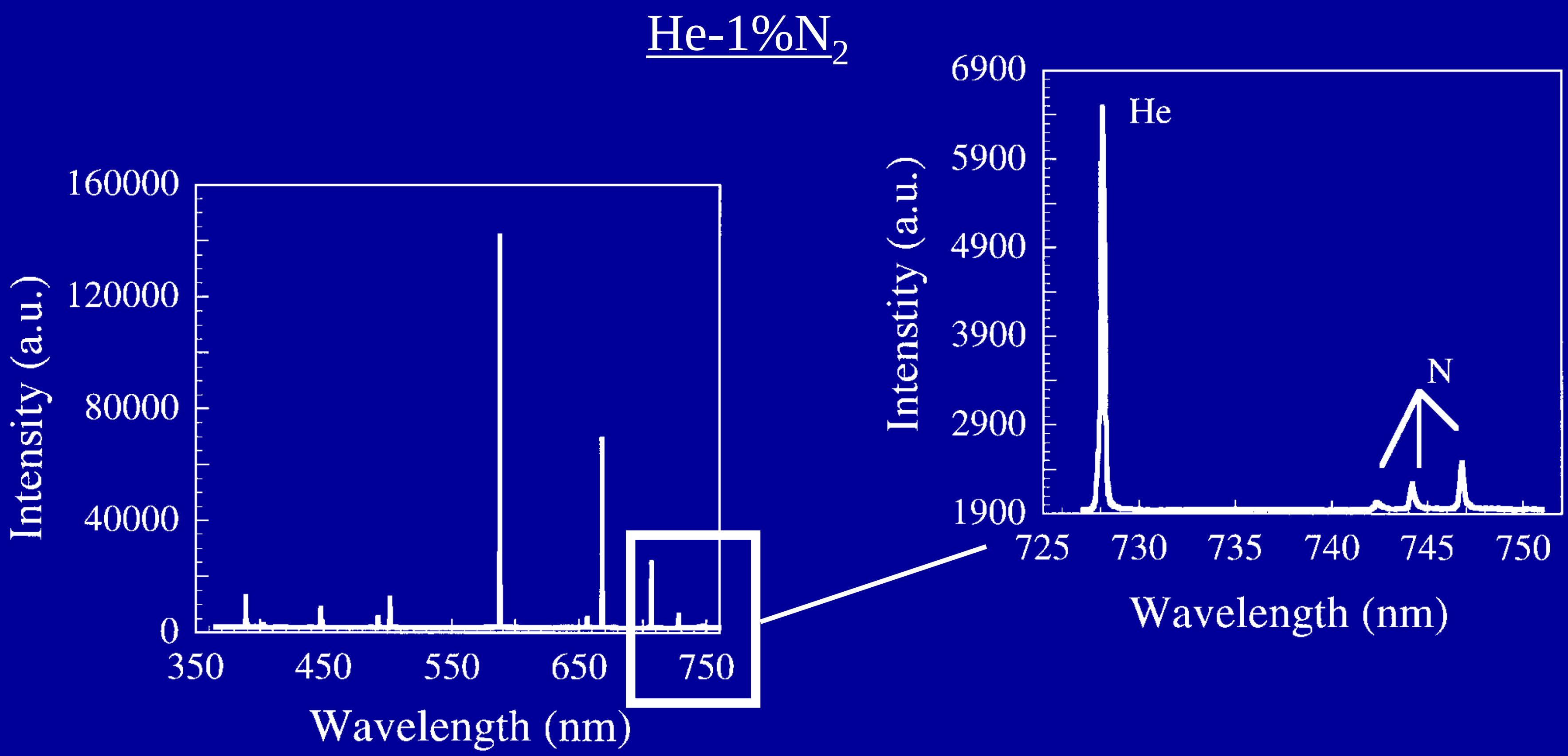

- **Experimental verification for the presence of species in the plasma phase.**

Nitrogen dissolution in the weld pool

Much higher than Sieverts' law values of nitrogen concentration can be predicted by a two temperature model

But how?

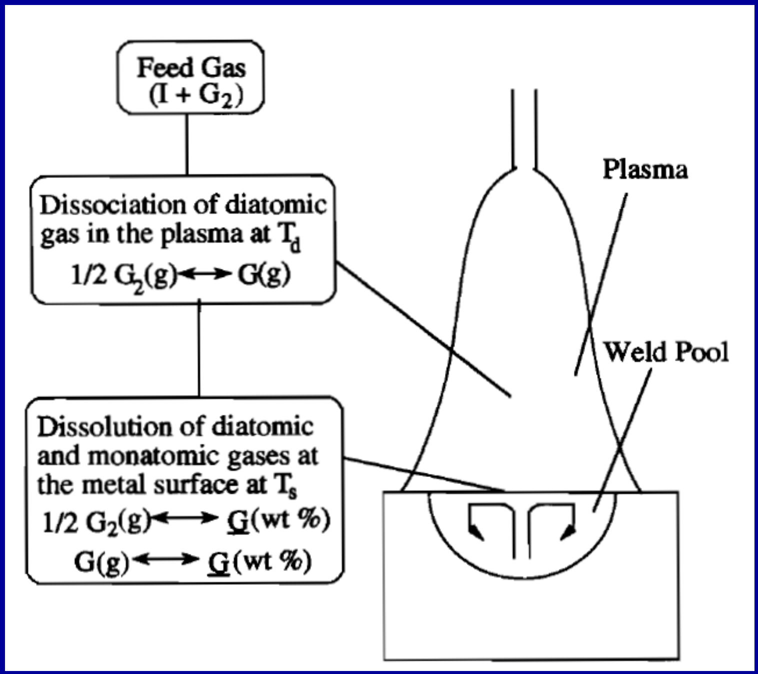

Two temperature model – useful and simple back of the envelop estimation of concentration

$$\underline{N}(\text{wt.\%}) = \sqrt{P_{N_2}}\ \exp\left(-\frac{1}{R}\left(\frac{\Delta G^{\circ}_{T_d}}{T_d} + \frac{\Delta G^{\circ}_{T_s}}{T_s}\right)\right)$$

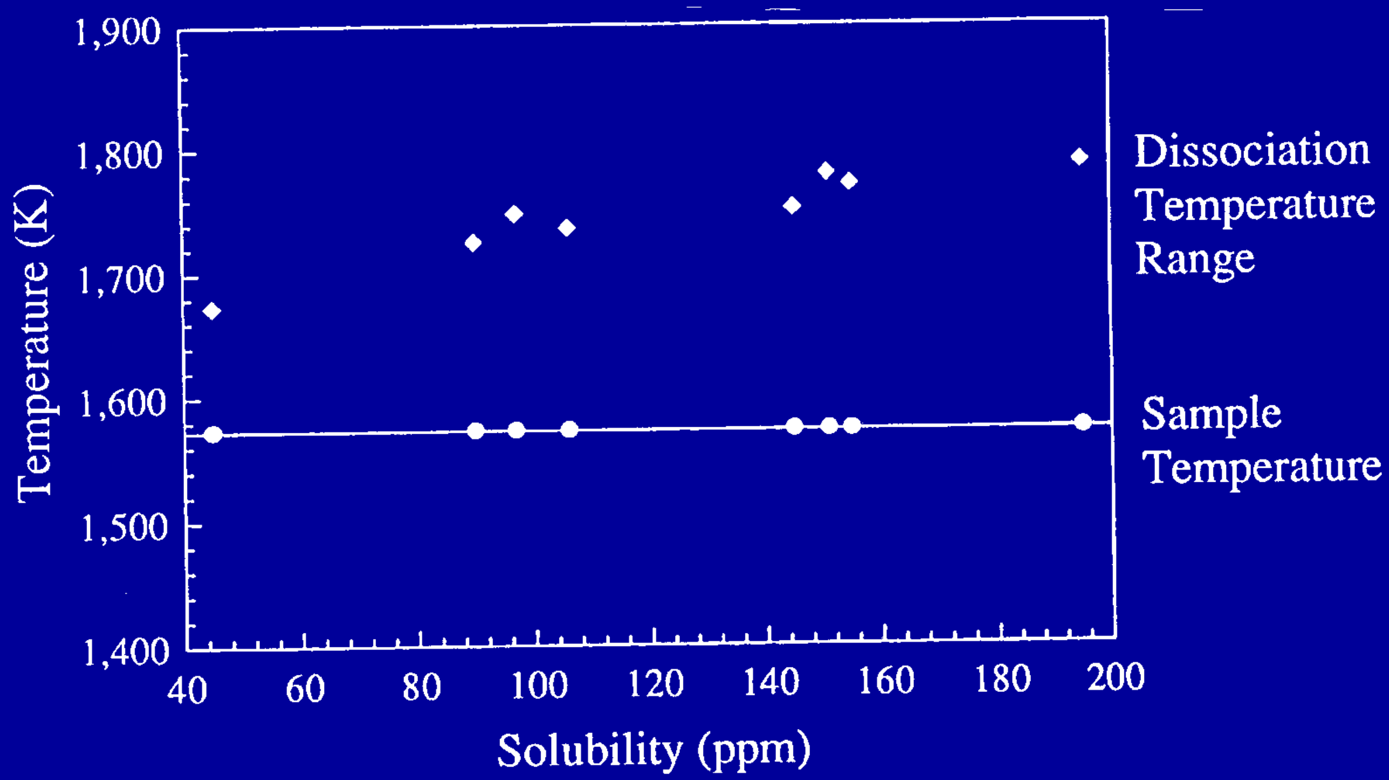

- Dissociation temperatures are 100-215 K above the sample temperature

But welds are not isothermal!

Nitrogen concentrations at the weld pool surface

Inside Arc Column

$$N(g) \rightarrow \underline{N}(ppm)$$

$$[\underline{N}] = P_N \exp\left(-\frac{\Delta G^\circ_{N(g)}}{RT}\right)$$

Outside Arc Column

$$\frac{1}{2}N_2(g) \rightarrow \underline{N}(ppm)$$

$$[\underline{N}] = \left(P_{N_2}\right)^{1/2} \exp\left(-\frac{\Delta G^\circ_{N_2(g)}}{RT}\right)$$

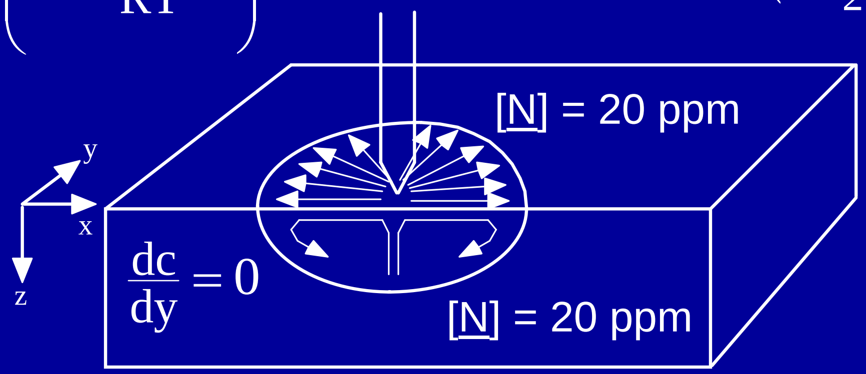

Reaction	Phase	Free Energy (J/mol)	Temperature Range (K)
$1/2\ N_2\ (g) \rightarrow N\ (g)$	gas	$362{,}318.0 - 65.52\ T$	273 to 1811
$N\ (g) \rightarrow \underline{N}$ (wt pct)	liquid	$-358{,}719.4 + 89.56\ T$	>1811
$N\ (g) \rightarrow \underline{N}$ (wt pct)	solid-δ	$-349{,}265.3 + 74.01\ T$	1663 to 1810
$N\ (g) \rightarrow \underline{N}$ (wt pct)	solid-γ	$-353{,}698.6 + 10.29\ T$	1185 to 1662
$N\ (g) \rightarrow \underline{N}$ (wt pct)	solid-α	$-349{,}265.3 + 74.01\ T$	273 to 1184
$1/2\ N_2\ (g) \rightarrow \underline{N}$ (wt pct)	liquid	$3598.2 + 23.89\ T$	>1811
$1/2\ N_2\ (g) \rightarrow \underline{N}$ (wt pct)	solid-δ	$13{,}052.4 + 8.49\ T$	1663 to 1810
$1/2\ N_2\ (g) \rightarrow \underline{N}$ (wt pct)	solid-γ	$-8619.0 + 37.40\ T$	1185 to 1662
$1/2\ N_2\ (g) \rightarrow \underline{N}$ (wt pct)	solid-α	$13{,}052.4 + 8.49\ T$	273 to 1184

Species concentrations in the plasma

$$Ar \rightarrow Ar^{+} + e^{-} \quad [1]$$

$$\frac{n_e n_{Ar^+}}{n_{Ar}} = \frac{2(2\pi m_e kT)^{3/2} Z_{Ar^+}}{h^3 \quad Z_{Ar}} e^{-(\varepsilon_{Ar})/kT} \quad [2]$$

$$Ar^{+} \rightarrow Ar^{++} + e^{-} \quad [3]$$

$$\frac{n_e n_{Ar^{++}}}{n_{Ar^+}} = \frac{2(2\pi m_e kT)^{3/2}}{h^3} \frac{Z_{Ar^{++}}}{Z_{Ar^+}} e^{-(\varepsilon_{Ar^+})/kT} \quad [4]$$

$$N_2 \rightarrow N_2^{+} + e^{-} \quad [5]$$

$$\frac{n_e n_{N_2^+}}{n_{N_2}} = \frac{2(2\pi m_e kT)^{3/2}}{h^3} \frac{Z_{N_2^+}}{Z_{N_2}} e^{-(\varepsilon_{N_2})/kT} \quad [6]$$

$$N \rightarrow N^{+} + e^{-} \quad [7]$$

$$\frac{n_e n_{N^+}}{n_N} = \frac{2(2\pi m_e kT)^{3/2}}{h^3} \frac{Z_{N^+}}{Z_N} e^{-(\varepsilon_N)/kT} \quad [8]$$

$$N_2(g) \rightarrow 2N(g) \quad [9]$$

$$K = \frac{p_N^2}{p_{N_2}} = \frac{(P)^2 (X_N)^2}{(P) X_{N_2}} = P \frac{(X_N)^2}{X_{N_2}} = \frac{(n_N)^2}{n_{N_2}} \left(\frac{RT}{N_A}\right) \quad [10]$$

$$n_e = n_{Ar^+} + 2n_{Ar^{++}} n_{N_2^+} + n_{N^+} \quad [11]$$

$$X_{Ar}\left(N_A\left(\frac{p}{RT}\right)\right) = X_{Ar}(n_{Ar} + 2n_{Ar^+} + 3n_{Ar^{++}}) \quad [12]$$

$$X_{N_2}\left(N_A\left(\frac{p}{RT}\right)\right) = X_{N_2}(n_{N_2} + 2n_{N_2^+} + n_N + 2n_{N^+}) \quad [13]$$

Species concentrations in Ar-5%N2 plasma

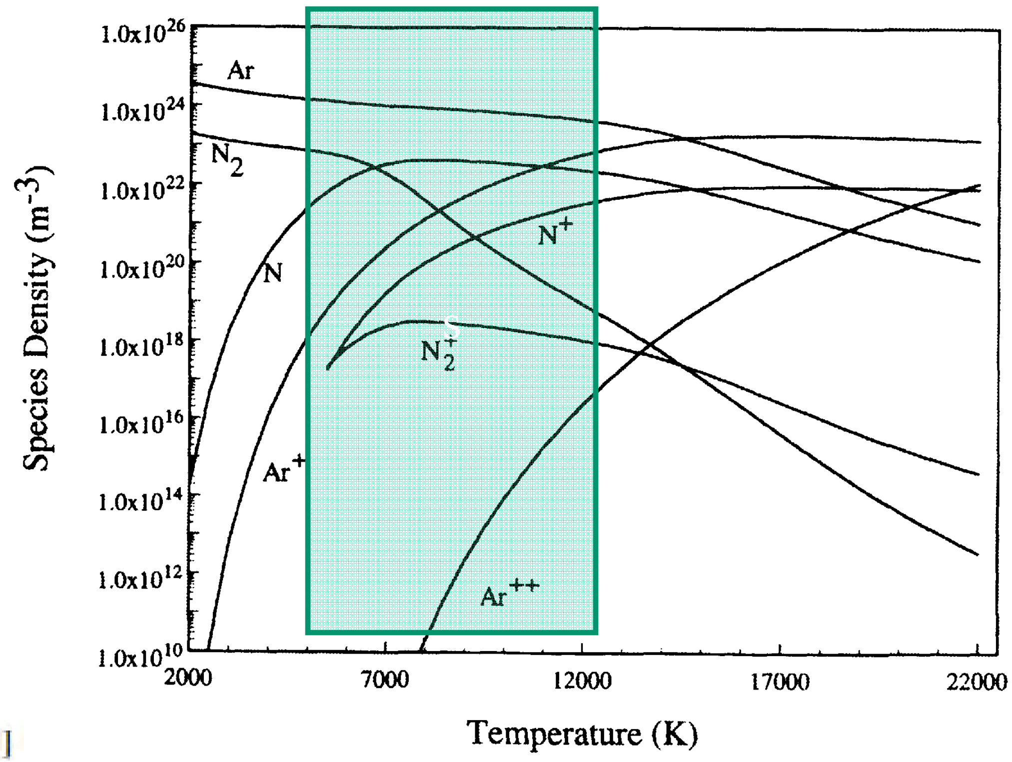

Important species: Ar, N2 and N

Calculation of nitrogen concentration **in the weld pool**

Main tasks:

Compute temperature and velocity fields in the weld pool

Compute species concentrations in the plasma above the weld pool

Compute nitrogen concentrations on the weld pool surface

Compute nitrogen concentrations in the entire specimen

Comparison between modeling and experimental results

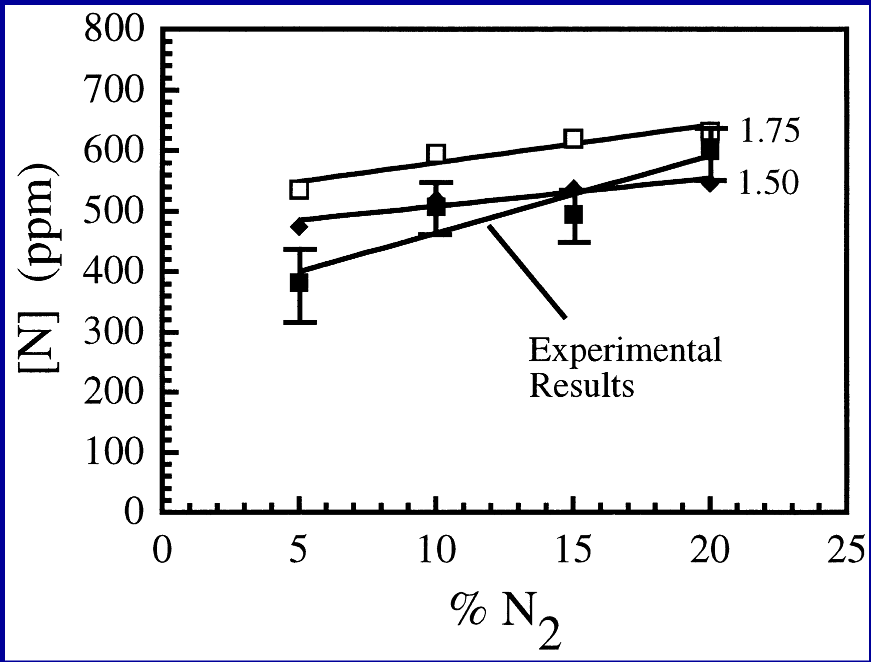

TRAVEL SPEED:
0.847 cm/sec

Modeled results with nitrogen supersaturations between 50 and 75% higher than Sieverts' Law calculations for $P(N_2)$ =1 atm correspond well with experimental results.

Many other applications

http://www.matse.psu.edu/modeling

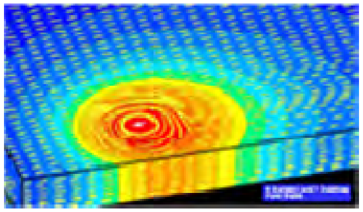 Flow and temperature fields in friction stir welding	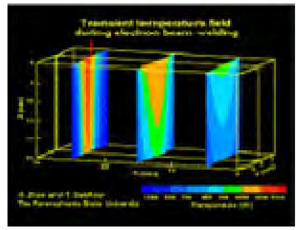 Keyhole mode welding	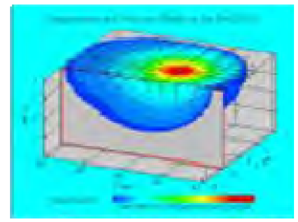 Weld pool temperature and velocity fields	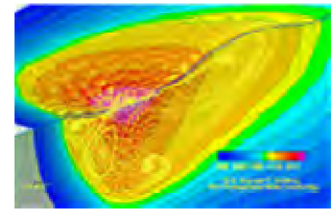 Liquid metal flow and free surface shape
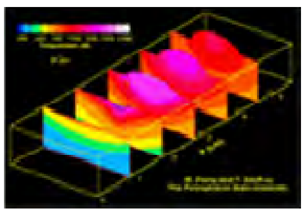 Bead shape development in GMA welding	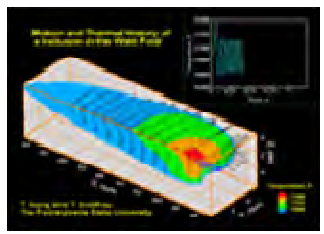 Inclusion motion in the weld pool	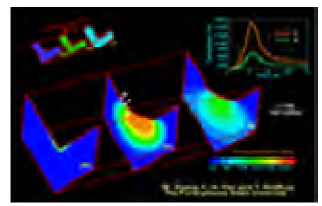 Fillet weld development and thermal cycle	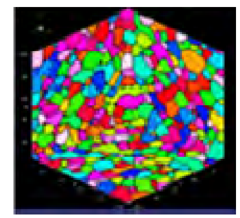 Monte Carlo simulation of isothermal grain growth
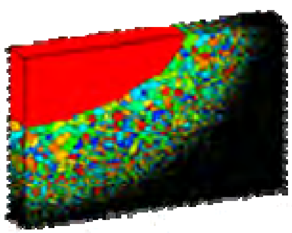 Grain growth during welding of Ti-6Al-4V	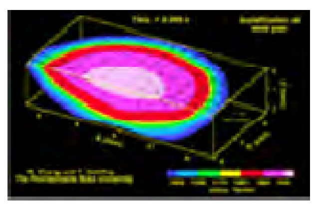 Cooling during spot welding	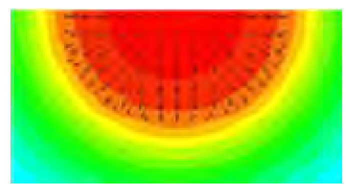 Heating and cooling of spot weld surface	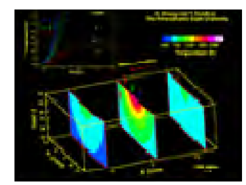 Phase transformation in 1005 steel during welding

From http://www.matse.psu.edu/modeling

Grain Growth in Ti-6Al-4V Heat Affected Zone

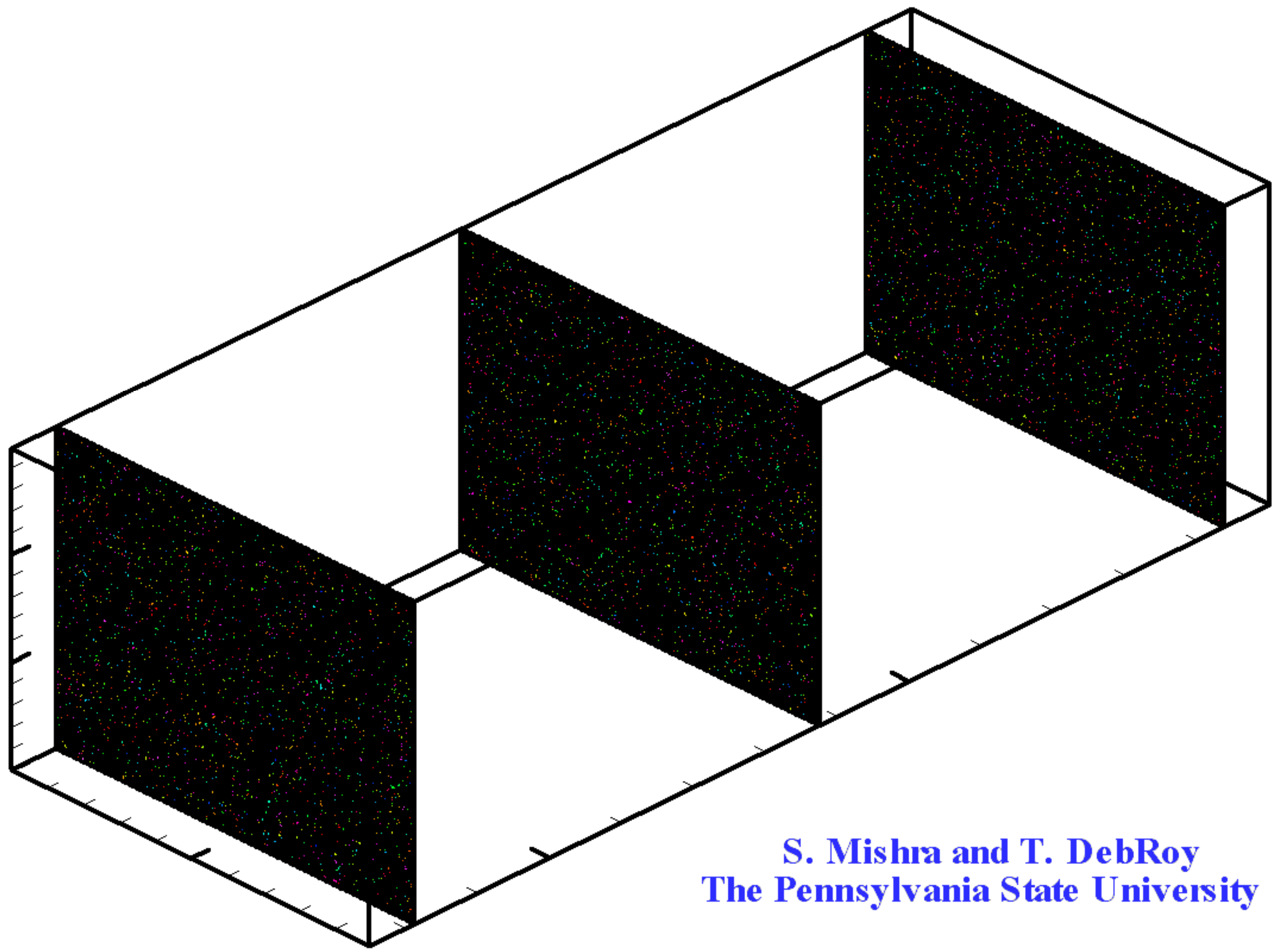

S. Mishra and T. DebRoy
The Pennsylvania State University

Tailoring weld geometry – has been done

Tailoring structure and properties?

Designer welds via multiple paths

Requirements: Geometry, cooling rate, or microstructure

Variable set 1

Variable set 2

Variable set 3

Variable set 4

Variable set 5

Variable set 6

Variable set 7

Variable set 8

Target weld geometry, cooling rate or other attributes

Tailoring weld geometry

Genetic Algorithm

Sets of $\left(\frac{I}{I_r}, \frac{V}{V_r}, \frac{U}{U_r}\right)$

Genetic algorithm

Calculated weld pool geometry

$$O2(f) = \left(\frac{p^c}{p^e} - 1\right)^2 + \left(\frac{w^c}{w^e} - 1\right)^2$$

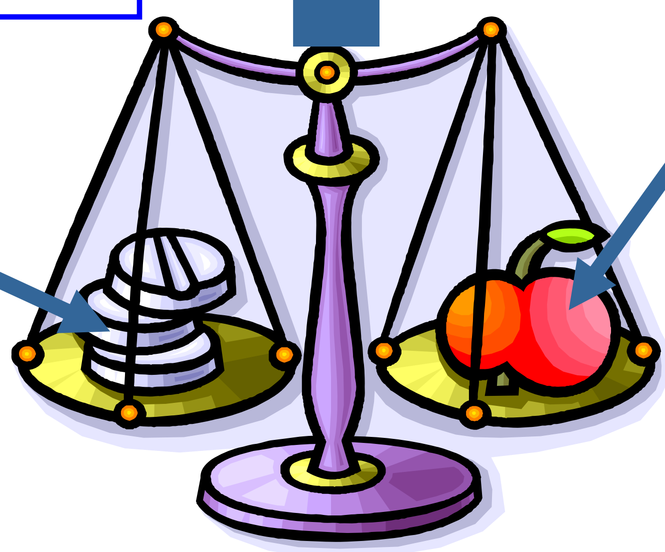

Desired weld pool geometry

Tailoring weld attributes

Target: Form a weld of the following dimensions:

Penetration : 1.23 mm Width : 4.47 mm

This weld was actually fabricated by GTA welding

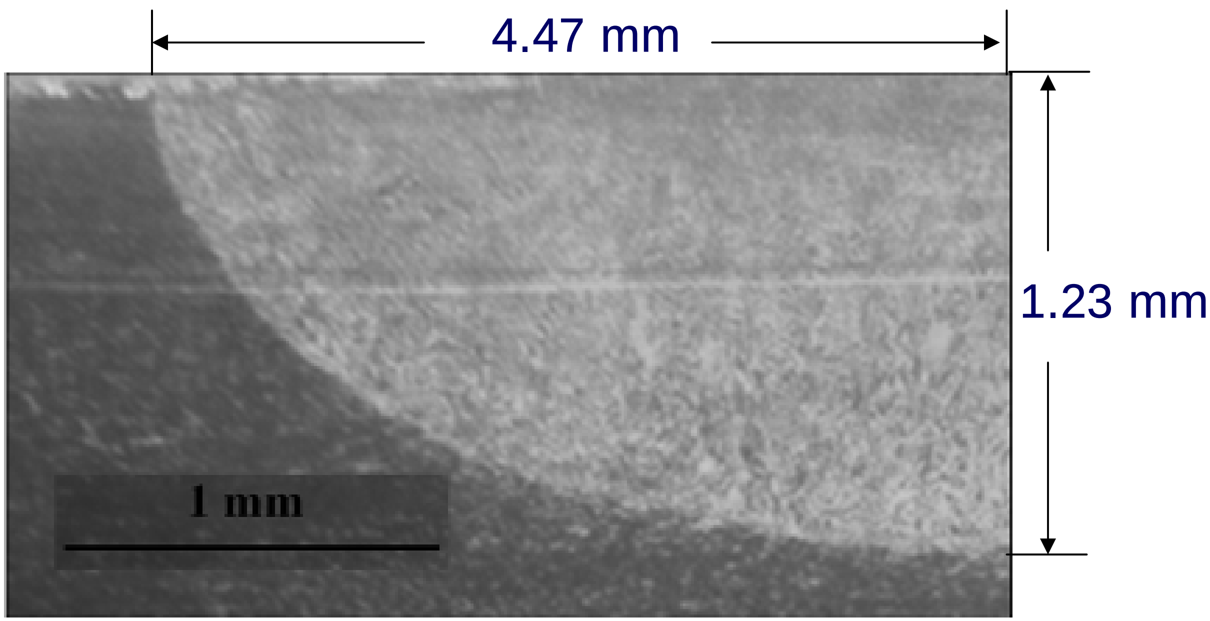

Current	140 A
Voltage	11.2 V
Welding Speed	7 mm/s

Bag, De and DebRoy, Materials and Manufacturing Processes., 2009

Objective function

$$O(f) = \left(\frac{w^{c} - w^{obs}}{w^{obs}}\right)^2 + \left(\frac{p^{c} - p^{obs}}{p^{obs}}\right)^2$$

W – weld pool width

P – weld pool penetration

Superscript c – computed values

Superscript obs – experimentally observed values

$$\{f\} \equiv \{\, f_1 \quad f_2 \quad f_3 \,\} = \left\{ \frac{I}{I_{mn}} \quad \frac{V}{V_{mn}} \quad \frac{v}{v_{mx}} \right\} = \{\, I^* \quad V^* \quad v^* \,\}$$

f – welding variable set

I – Current

V - Voltage

v – welding speed

Subscript mn– minimum allowed value

Subscript mx – maximum allowed value

Bag, De and DebRoy, Materials and Manufacturing Processes., 2009

Objective function with I^*, V^* and v^*

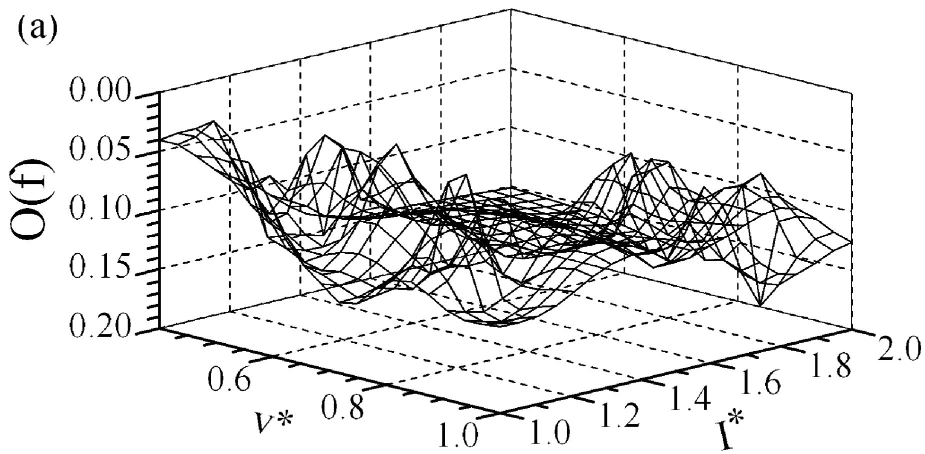

O(f) for the initial population

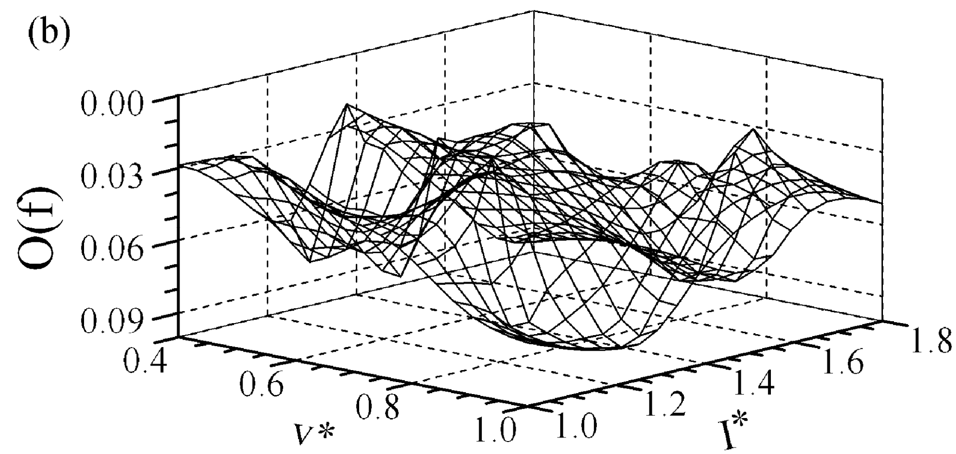

O(f) after ten generations

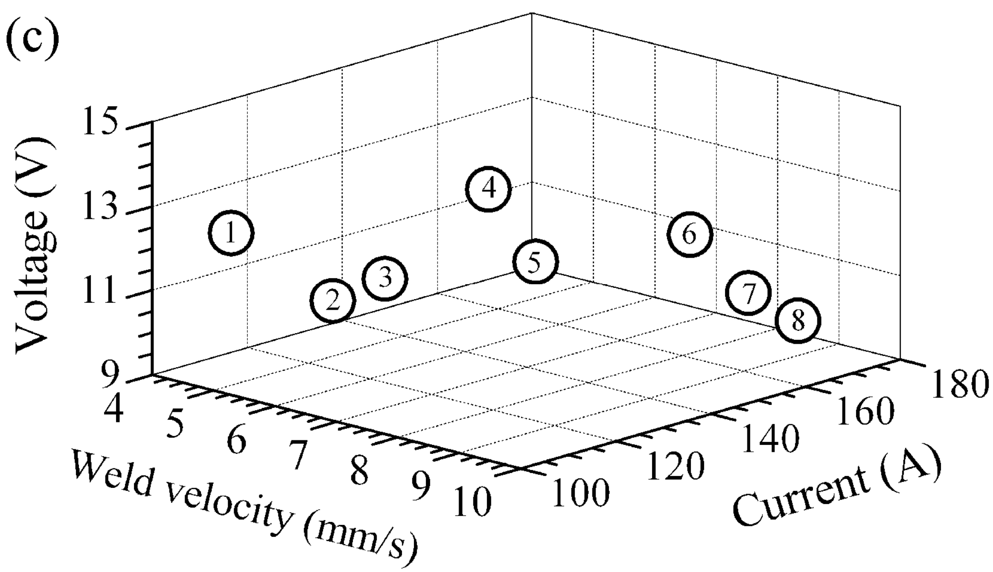

Eight alternate welding conditions achieved after fifteen generations

Bag, De and DebRoy, Materials and Manufacturing Processes., 2009

Multiple combinations of welding parameters result in roughly the same target geometry

Target geometry: penetration = 1.23 mm, width = 4.47 mm

I = 140 A, V = 11.2 V, Welding speed = 7 mm/s

Individual solutions	I (amp)	V (Volt)	U (mm/s)	Penetration (mm)	Width (mm)
(1)	134	9.8	4.3	1.24	4.54
(2)	140	11.5	7.1	1.24	4.57
(3)	135	10.6	5.1	1.25	4.60
(4)	163	10.3	9.6	1.18	4.34
(5)	117	14.4	8.2	1.23	4.53
(6)	149	12.6	9	1.28	4.63
(7)	106	12.5	4.8	1.23	4.45
(8)	166.5	10.5	8.6	1.24	4.55

Bag, De and DebRoy, Materials and Manufacturing Processes., 2009

Geometries of fabricated welds

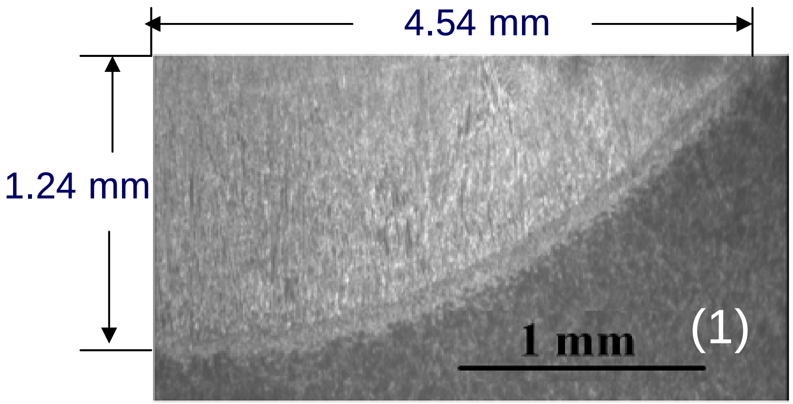

134 A, 9.8 V, 4.3 mm/s

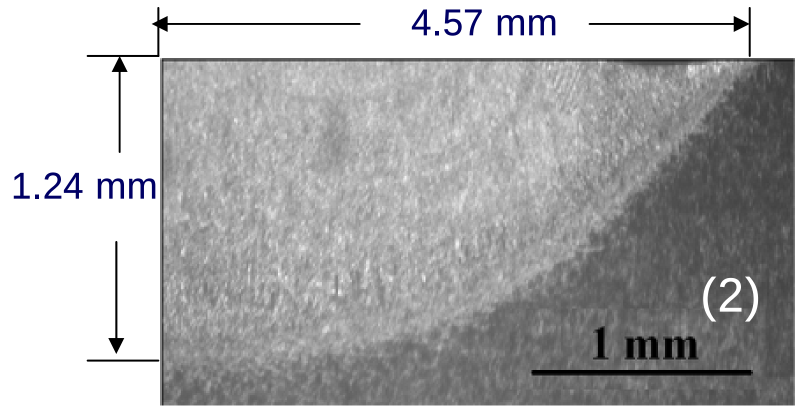

140 A, 11.5 V, 7.1 mm/s

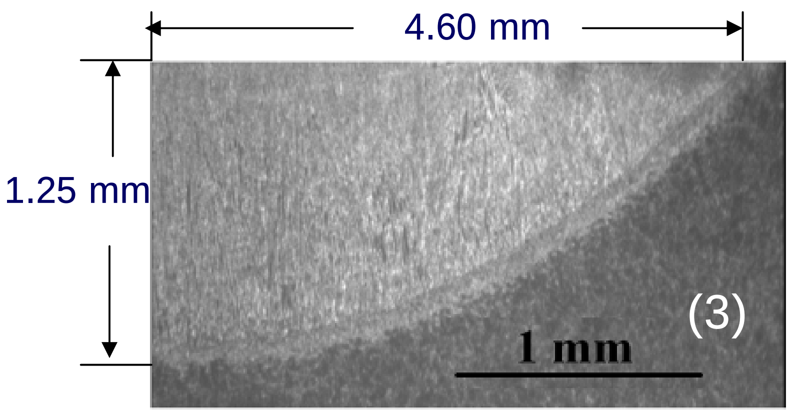

135 A, 10.6 V, 5.1 mm/s

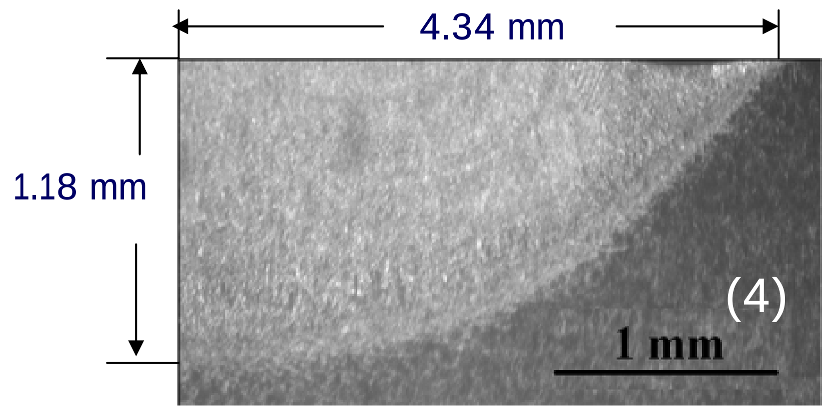

163 A, 10.3 V, 9.6 mm/s

Bag, De and DebRoy, Materials and Manufacturing Processes., 2009

Geometries of fabricated welds

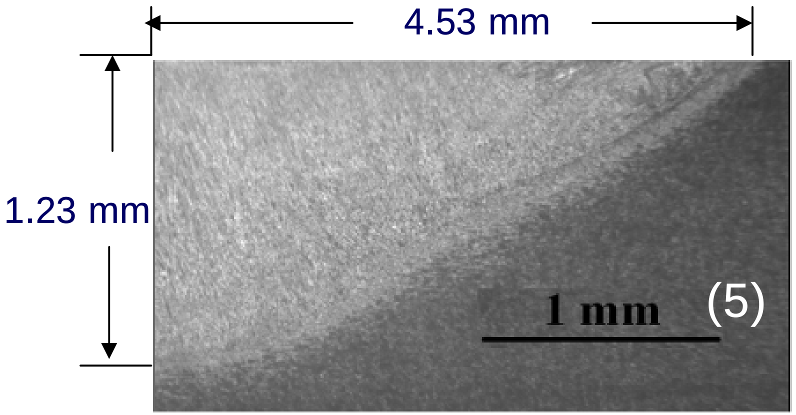

117 A, 14.4 V, 8.2 mm/s

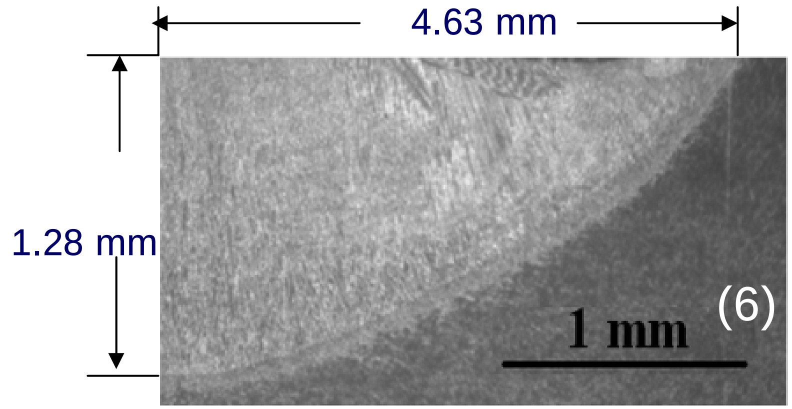

149 A, 12.6 V, 9 mm/s

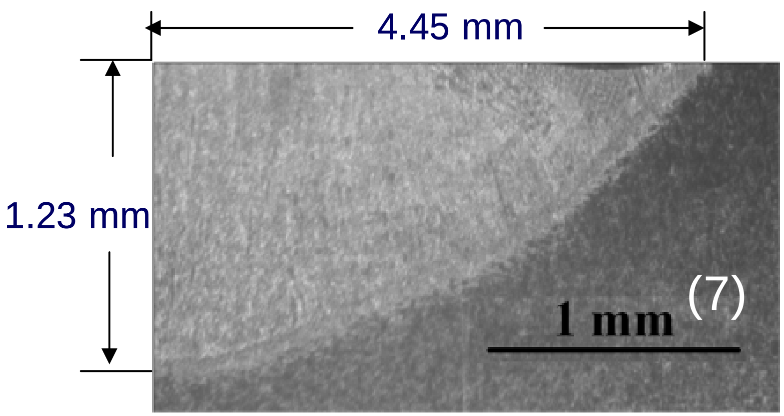

106 A, 12.5 V, 4.8 mm/s

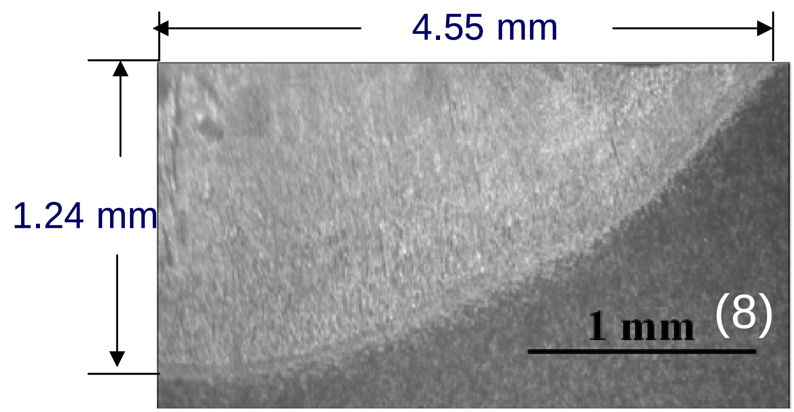

166.5 A, 10.5 V, 8.6 mm/s

Bag, De and DebRoy, Materials and Manufacturing Processes., 2009

Multiple sets of welding variables can produce a target geometry

Arc welding of SS304 to produce 4.47 mm wide and 1.23 mm deep pool

Obtained by GA | **Obtained by experiments**

Current (A)	Voltage (V)	Velocity (mm/s)	Width (mm)		Penetration (mm)	
			computed	measured	computed	measured
134.0	9.8	4.3	4.54	4.81	1.24	1.20
140.3	11.5	7.1	4.57	4.89	1.24	1.21
134.8	10.6	5.1	4.60	4.78	1.25	1.27
163.0	10.3	9.6	4.34	4.60	1.18	1.22
117.0	14.4	8.2	4.53	4.23	1.23	1.19
149.0	12.6	9.0	4.63	4.90	1.28	1.30
106.1	12.5	4.8	4.45	4.26	1.23	1.21
166.5	10.5	8.6	4.55	4.65	1.24	1.25

Thank you very much

More models, animations and papers at http://www.matse.psu.edu/modeling